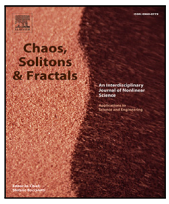
Chaos, Solitons and Fractals 189 (2024) 115719



Contents lists available at ScienceDirect

Chaos, Solitons and Fractals

journal homepage: www.elsevier.com/locate/chaos





Analysis of an opinion dynamics model coupled with an external environmental dynamics☆

Anthony Couthures [a,*], Vineeth Satheeskumar Varma [a,b], Samson Lasaulce [a,c], Irinel - Constantin Morărescu [a,b]

[a] Université de Lorraine, CNRS, CRAN, Nancy, F-54000, France
[b] Automation Department, Technical University of Cluj-Napoca, Cluj-Napoca, Romania
[c] Khalifa University, Abu Dhabi, United Arab Emirates

ARTICLE INFO

Keywords:
Complex networks
Opinion dynamics
Bifurcations
Chaotic systems
Limit cycles

ABSTRACT

We consider a set of individuals, referred to as agents, whose opinions evolve according to nonlinear dynamics. Their opinions impact their behavior or actions, which in turn affect their local environment (for example, via pollution, contamination of a virus, etc.). Each agent can also perceive or observe a signal about the environment, and is influenced by this external signal. This yields a coupled dynamics (opinion and external signal), which behaves in a similar manner to the prey–predator models. One of the main features of our study is that the information provided by the external signal has a significant impact on the opinion dynamics. When the coupling is strong, the external signal may induce either chaotic behavior or convergence towards a limit cycle. When the coupling with the external signal is weak, the classical behavior characterized by local agreements in polarized clusters is observed. In both cases, conditions under which clusters of individuals do not change their actions are provided. Numerical examples are provided to illustrate the derived analytical results.

1. Introduction

Opinion dynamics (OD) over social networks is a topic that has received increasing attention during the last few decades. One effective way to model OD under social interactions is through multi-agent systems formalism. Several OD models exist, and they can be split in different ways. The first one assumes that opinions evolve in a discrete set of values [1,2] while others consider that opinions lie in a continuous set of values [3–6]. While some models naturally lead to consensus [5,7], others yield network clustering [3,4,6,8]. A common feature of all the models enumerated above is that each individual has access to the exact opinion values of its neighbors. This assumption is not realistic, and to overcome it, a mix of continuous opinion with discrete actions (CODA) was proposed in [9]. This model reflects the fact that even if we often face binary choices or actions that are visible to our neighbors, our opinion evolves in a continuous space of values that are not accessible. A consensus-like dynamics reproducing this behavior has been proposed and analyzed in [10] where the preservation and propagation of actions are also characterized through the notion of robust polarized clusters. While the model in [10] led to a clustering of the network, a similar idea was employed in [11] to study the emergence of consensus under quantized all-to-all communication.

In this paper, we analyze the behavior of a slightly generalized CODA model coupled with the dynamics of an external environmental state, which represents, in this work, the atmospheric pollution levels. It is noteworthy that our results can be adapted to other scenarios in which the external signal describes virus contamination or marketing instances. The usage of the CODA model for opinion dynamics is justified by two important social features: (1) individuals may have access to an inexact/quantized perception of the opinion of their neighbors, (2) the extremists are more stubborn and their opinion is more difficult to change. Many models have been developed to characterize the atmospheric pollution dynamics [12]. One of the popular modeling approaches is based on the half-life decomposition of polluting compounds (see, for instance, [13,14]). Generally, the time constants of the processes depend on the chemical compound considered [14,15] and the dynamics may be cumbersome. Since our focus is not on the precise modeling of this process, we use a simple linear pollution model to describe the evolution of the environmental air pollution. In this model, the state of the environment depends on the states (capturing

☆ This work was supported by project DECIDE funded under the PNRR I8 scheme by the Romanian Ministry of Research.
* Corresponding author.
E-mail address: anthony.couthures@univ-lorraine.fr (A. Couthures).

https://doi.org/10.1016/j.chaos.2024.115719
Received 19 July 2024; Received in revised form 25 September 2024; Accepted 31 October 2024
Available online 16 November 2024
0960-0779/© 2024 Elsevier Ltd. All rights are reserved, including those for text and data mining, AI training, and similar technologies.

the environmental behavior) of the individuals, which in turn are influenced both by the states of their neighbors and the external signal (pollution level). The coupling of the two dynamics leads to a complex asymptotic behavior that can be summarized as follows: When the coupling between the dynamics is weak, one recovers the asymptotic behavior similar to the CODA model in [10] or to [16]. A strong coupling between the two dynamics hampers the convergence towards a steady state and yields either chaotic oscillation or convergence towards a limit cycle. It is noteworthy that even in the simplified case, when all the agents have the same initial opinion, the strong coupling with the external dynamics hampers the convergence towards a steady state and may lead to chaotic oscillations. As shown in the sequel, our model behaves as a prey–predator model where the predators thrive when the prey thrive, but this leads to the decline of the prey, which in turn yields the decline of the predators [17,18].

We point out that the idea of coupling environment dynamics and population behavior is not new, it has been mainly studied in the framework of evolutionary games [19–21]. While these studies also emphasize similar oscillatory asymptotic behavior, they employ different tools and the insights are different. For example, in [19–21] the propagation of the information is homogeneous (the entire population gets the same information) and the oscillations are induced by the time-varying proportion of the population adopting one of the two possible strategies. In our case, the information propagates through a graph of individuals with different stubbornness and the oscillations are induced by the pollution level that triggers different social behaviors.

The main contributions of this paper are: (i) the introduction of a mathematical model capturing the coupling between a nonlinear opinion dynamics model and an external signal; (ii) the analysis of the asymptotic behavior of the aforementioned model. Those contributions follow from the work initiated in [22]. Note that both the opinion dynamics and the pollution dynamics models are inspired by existing works in the literature.

The paper is structured as follows: Section 2 introduces the main notions and concepts necessary to describe the mathematical model that is analyzed in the sequel. Characteristics of equilibrium and asymptotic behavior are analyzed in Section 3. Section 5 numerically highlights various setups leading to different asymptotic behaviors. The manuscript ends with Section 6 which presents concluding remarks about the work.

In the following, $\mathbb{R}$ and $\mathbb{R}_{\geq 0}$ denote the set of real numbers and non-negative real numbers, respectively. We will use the notation for the identity matrix $\mathbf{I} \in \mathbb{R}^{N\times N}$ when there is no ambiguity. For the specific case of dimension $n \in \mathbb{N}$, we denote the identity matrix as $\mathbf{I}_n \in \mathbb{R}^{n\times n}$. The scalar identity function is denoted as $\mathrm{Id} : \mathbb{R} \to \mathbb{R}$, where $\mathrm{Id}(x) = x$. Moreover, we denote by $\mathbf{1}$ the all-ones vector and by $\mathbf{0}$ the null vector in $\mathbb{R}^N$ when there is no ambiguity, and for the n-dimensional cases, $\mathbf{1}_n$ and $\mathbf{0}_n$ respectively. In the sequel, for $i \in \mathcal{V}$, e_i denotes the ith element of the canonical basis of $\mathbb{R}^N$. For a function $f : X \to X$, we denote by $\mathrm{Fix}(f) \subset X$ the set of fixed points of f, i.e., $\mathrm{Fix}(f) := \{x \in X \mid f(x) = x\}$.

2. Problem formulation and preliminaries

We consider the classical multi-agent framework in which N individuals/agents belonging to the set $\mathcal{V} = \{1, \dots, N\}$ and interacting according to a fixed *directed graph* $\mathcal{G} = (\mathcal{V}, \mathcal{E})$ which does not contains loop. We denote by $\boldsymbol{A} \in \mathbb{R}_+^{N\times N}$ its adjacency matrix, such that $A_{ij} = 1$ if $(i, j) \in \mathcal{E}$ and 0 otherwise, by $\boldsymbol{D} \in \mathbb{R}^{N\times N}$ its degree matrix and by $\boldsymbol{L} \in \mathbb{R}^{N\times N}$ where $\boldsymbol{L} = \boldsymbol{D} - \boldsymbol{A}$ the associated Laplacian. The neighborhood of the agent i is denoted by $\mathcal{N}_i$ and represents the set of agents that influence i according to the graph $\mathcal{G}$ (i.e $j \in \mathcal{N}_i \Leftrightarrow (j, i) \in \mathcal{E}$). We denote by n_i the cardinality of $\mathcal{N}_i$. Let us also recall that a path in $\mathcal{G}$ is a finite sequence of edges $(i_1, i_2), (i_2, i_3), \dots, (i_p, i_{p+1})$ such that $(i_k, i_{k+1}) \in \mathcal{E}$ for all $k \in \{1, \dots, p\}$. Two vertices i, $j \in \mathcal{V}$ are *connected* in $\mathcal{G}$ if there exists a path in $\mathcal{G}$ joining i and j (i.e. $i_1 = i$ and $j_p = j$). Finally, a directed graph $\mathcal{G}$ is strongly connected if any two nodes in $\mathcal{V}$ are connected.

At each time instant $k \in \mathbb{N}$ we assign to each agent $i \in \mathcal{V}$ an opinion $\theta_i(k) \in \Theta := [-1, 1]$ that evolves according to the discrete-time protocol defined further in (2). We also introduce $\boldsymbol{\theta}(k) = \left(\theta_i(k)\right)_{i\in\mathcal{V}} \in \boldsymbol{\Theta} := [-1, 1]^N$ the vector collecting the opinions of all the agents at time k. Note that $\theta_i(k)$ is an abstraction which is closer to -1 when the individual i is more convinced to have a pro-environmental behavior and closer to 1 when the individual does not care about the environment and behaves accordingly. We assume that the only information from the neighbors is the behavior/action captured by the monotonically increasing function $s_\theta : \Theta \to \Theta$ as a proxy of θ_i and verifying $s_\theta(-1) = -1$ and $s_\theta(1) = 1$. Let us denote $\boldsymbol{s}_\theta(\boldsymbol{\theta}) = \left(s_\theta\left(\theta_i\right)\right)_{i\in\mathcal{V}}$.

Remark 1. Note that s_θ can be the identity function meaning that the agents can access the actual opinions of their neighbors. The other extreme case is when s_θ is when the sign function in which the agents can only detect if the neighbors are above or below the average of the eco-responsibility. Moreover, the intermediate situation is also possible with s_θ being a smooth sigmoid function like $s_\theta(\theta) = 2\arctan(m\theta/(1-\theta^2))/\pi$ with $m \in \mathbb{N}$ a parameter allowing to change the steepness of the curve.

We assume that the opinion of agent i at time k induces a behavior generating certain emissions, which are captured by the increasing function $E : \Theta \to \left[e_{\min}, e_{\max}\right]$ where $0 < e_{\min} < e_{\max}$ are the minimum and maximum emissions, respectively. For simplicity, we note the emission of agent i at time k with $E\left(\theta_i(k)\right)$. Also, we denote by $\boldsymbol{E}(\boldsymbol{\theta}) = \left(E\left(\theta_i\right)\right)_{i\in\mathcal{V}}$ the vector of emission of all the agents.

The state of the environment is characterized by another abstraction, $p \in \mathbb{R}_{\geq 0}$, that captures the pollution state under the emission of the overall network of individuals. To keep things simple, we assume that the pollution evolves according to the following discrete-time dynamics:

$$\begin{aligned} p(k+1) &= (1-\gamma)\, p(k) + \sum_{i=1}^{N} E(\theta_i(k)) \\ &= (1-\gamma)\, p(k) + \mathbf{1}^\top \boldsymbol{E}(\boldsymbol{\theta}(k)), \end{aligned} \tag{1}$$

where $\gamma \in (0, 1)$ is an autonomous decay rate. This dynamics is taken as a simplification of Eq. (2) of [14].

We also assume that individuals cannot observe p accurately, instead, they can perceive an output of the environmental dynamics defined by the function $s_p : \mathbb{R} \to \Theta$. The output s_p of the air pollution is relative to a deviation from a threshold denoted $\bar{p} \in \mathbb{R}_{\geq 0}$. Basically, the population will perceive a polluted environment if $p > \bar{p}$ and will have the feeling that air is healthy otherwise. The function s_p is increasing with respect to the difference $\bar{p} - p$ and such that $s_p(q) = 0$ if and only if $q = 0$.

We also state the following standing assumption:

Standing Assumption 1. For $\gamma \in (0, 1)$ such as in (1), we have $Ne_{\min}/\gamma < \bar{p} < Ne_{\max}/\gamma$.

This assumption allows us to exclude the case when the external signal has no significant influence on the opinion dynamics. When this assumption is not satisfied the analysis reduces to the OD dynamics, as even when all the agents are polluting (or not), the air pollution signal remains below (or above) the threshold. Further details on this case can be found in [22].

We are now ready to describe the OD model that we consider in this work. This dynamics adapts the CODA model in [10,16] to include the external dynamics of $p(k)$:

$$\begin{aligned} \theta_i(k+1) = \theta_i(k) + \left(1-\theta_i(k)^2\right) \Big[& \beta\left(s_p(\bar{p} - p(k)) - \theta_i(k)\right) \\ & + (1-\beta)\frac{1}{n_i}\sum_{j\in\mathcal{N}_i}\left(s_\theta(\theta_j(k)) - \theta_i(k)\right)\Big], \end{aligned} \tag{2}$$

where $0 < \beta < 1$ encapsulates the trade-off between the external signal and the neighbors' behavior on the opinion evolution.

Noting the state as $\boldsymbol{x}(k) = (\boldsymbol{\theta}(k), p(k))$, we can rewrite (1) and (2) in the collective form as:

$$\boldsymbol{x}(k+1) = \mathbf{F}(\boldsymbol{x}(k)) = \begin{pmatrix} \boldsymbol{u}(\boldsymbol{\theta}(k), p(k)) \\ \upsilon(\boldsymbol{\theta}(k), p(k)) \end{pmatrix}, \tag{3}$$

where the functions are,

$$\boldsymbol{u}(\boldsymbol{\theta}, p) = \boldsymbol{\theta} + \left(\mathbf{I} - \operatorname{diag}(\boldsymbol{\theta})^2\right)(\boldsymbol{f}(\boldsymbol{\theta}, p) - \boldsymbol{\theta}),$$

$$\upsilon(\boldsymbol{\theta}, p) = (1-\gamma)\, p + \mathbf{1}^\top \boldsymbol{E}(\boldsymbol{\theta}),$$

and

$$\boldsymbol{f}(\boldsymbol{\theta}, p) = \beta s_p(\bar{p} - p)\mathbf{1} + (1-\beta)\, \boldsymbol{D}^{-1} \boldsymbol{A} s_\theta(\boldsymbol{\theta}).$$

Having established the foundational dynamics model, we now turn to a detailed analysis of its behavior.

3. Analysis of the general case

This section delves into an analysis of the model's dynamics, beginning with the characterization of equilibria in the general case and incorporating results that exploit the graph structure. Subsequently, we examine the stability of certain equilibrium points located at the extremes of the state space. Additionally, we explore scenarios involving fully synchronized opinions and study the system's equilibria under piece-wise linear signals.

But first, the following general invariance result can be stated.

Lemma 1. *The compact set $\mathcal{X} = \boldsymbol{\Theta} \times \left[N e_{min}/\gamma, N e_{max}/\gamma\right]$ is forward invariant under the dynamics (3). i.e. $\forall \boldsymbol{x} \in \mathcal{X}$, $\boldsymbol{F}(\boldsymbol{x}) \in \mathcal{X}$.*

Proof. Note that $\boldsymbol{f}(\boldsymbol{\theta}, p)$ is the convex combination of two vectors in $\boldsymbol{\Theta}$. Thus, for all $(\boldsymbol{\theta}, p) \in \boldsymbol{\Theta} \times \mathbb{R}_{\geq 0}$ and for any $i \in \mathcal{V}$ one obtains,

$$-1 \leq e_i^\top \boldsymbol{f}(\boldsymbol{\theta}, p) \leq 1 \Leftrightarrow -1 - \theta_i \leq e_i^\top \boldsymbol{f}(\boldsymbol{\theta}, p) - \theta_i \leq 1 - \theta_i,$$

which implies:

$$-1 \leq e_i^\top \boldsymbol{u}(\boldsymbol{\theta}, p) \leq 1 \Leftrightarrow \boldsymbol{u}(\boldsymbol{\theta}, p) \in \boldsymbol{\Theta}.$$

Furthermore, for any $\boldsymbol{\theta} \in \boldsymbol{\Theta}$, the inequality $N e_{\min} < \boldsymbol{E}(\boldsymbol{\theta}) < N e_{\max}$ holds. Then, for any $(\boldsymbol{\theta}, p) \in \mathcal{X}$, one has,

$$\begin{aligned} &\frac{N e_{\min}}{\gamma} < p < \frac{N e_{\max}}{\gamma} \\ \Leftrightarrow\ & (1-\gamma)\frac{N e_{\min}}{\gamma} + N e_{\min} < \upsilon(\boldsymbol{\theta}, p) < (1-\gamma)\frac{N e_{\max}}{\gamma} + N e_{\max} \\ \Leftrightarrow\ & \frac{N e_{\min}}{\gamma} < \upsilon(\boldsymbol{\theta}, p) < \frac{N e_{\max}}{\gamma}. \end{aligned}$$

Therefore, for any $\boldsymbol{x} \in \mathcal{X}$, it follows that $\boldsymbol{F}(\boldsymbol{x}) \in \mathcal{X}$. □

This Lemma ensures the forward invariance of the compact set $\mathcal{X}$ under the dynamics (3), meaning that for every trajectory $(x(k))_{k\in\mathbb{N}}$ such that there exists a $k \in \mathbb{N}$ with $x(k) \in \mathcal{X}$, then for all $l \in \mathbb{N}$, it follows that $x(k+l) \in \mathcal{X}$. Additionally, it can be observed that $\mathcal{X}$ is attractive with respect to the environment dimension, meaning that for any $x(0) \in \boldsymbol{\Theta} \times \mathbb{R}_{\geq 0}$, there exists a time $k \in \mathbb{N}$ such that $\boldsymbol{x}(k) \in \mathcal{X}$.

3.1. Characterization of equilibria

We start with the characterization of the equilibria of (3) i.e., the points $\boldsymbol{x}^*$ such that $\boldsymbol{x}^* = \mathbf{F}(\boldsymbol{x}^*)$ or $\boldsymbol{x}^* \in \operatorname{Fix}(\boldsymbol{F})$. Before introducing the following result let us define the instrumental function $\boldsymbol{g} : \boldsymbol{\Theta} \to \boldsymbol{\Theta}$ such that

$$\boldsymbol{g}(\boldsymbol{\theta}) = \beta s_p\left(\bar{p} - \frac{\mathbf{1}^\top \boldsymbol{E}(\boldsymbol{\theta})}{\gamma}\right)\mathbf{1} + (1-\beta)\, \boldsymbol{D}^{-1} \boldsymbol{A} s_\theta(\boldsymbol{\theta}). \tag{4}$$

Proposition 1. *Let $\boldsymbol{x}^* = (\boldsymbol{\theta}^*, p^*)$ be an equilibrium point of the dynamics (3). Then, $\boldsymbol{x}^* = \left(\boldsymbol{\theta}^*, \mathbf{1}^\top \boldsymbol{E}(\boldsymbol{\theta}^*)/\gamma\right)$ such that $\boldsymbol{\theta}^* \in \mathcal{F}$ with*

$$\mathcal{F} = \left\{(\theta_i)_{i\in\mathcal{V}} \in \boldsymbol{\Theta} \mid \forall i \in \mathcal{V},\ \theta_i \in \{-1, 1\} \ \text{ or } \theta_i = e_i^\top \boldsymbol{g}(\boldsymbol{\theta})\right\}. \tag{5}$$

Proof. Assuming that $\boldsymbol{x}^*$ is an equilibrium of (3) it is straightforward to see from (1) that

$$p^* = \upsilon(\boldsymbol{\theta}^*, p^*) \Leftrightarrow p^* = (1-\gamma)\, p^* + \mathbf{1}^\top \boldsymbol{E}(\boldsymbol{\theta}^*) \Leftrightarrow p^* = \frac{\mathbf{1}^\top \boldsymbol{E}(\boldsymbol{\theta}^*)}{\gamma}.$$

Injecting the expression of p^* into the equation $\boldsymbol{\theta}^* = u(\boldsymbol{\theta}^*, p^*)$, one obtains,

$$u\left(\boldsymbol{\theta}^*, \frac{\mathbf{1}^\top \boldsymbol{E}(\boldsymbol{\theta}^*)}{\gamma}\right) - \boldsymbol{\theta}^* = \mathbf{0}.$$

Which is equivalent to,

$$\begin{aligned} &\left(\mathbf{I} - \operatorname{diag}(\boldsymbol{\theta}^*)\right)\left(\mathbf{I} + \operatorname{diag}(\boldsymbol{\theta}^*)\right) \times \\ &\underbrace{\left(\beta s_p\left(\bar{p} - \frac{\mathbf{1}^\top \boldsymbol{E}(\boldsymbol{\theta}^*)}{\gamma}\right)\mathbf{1} + (1-\beta)\, \boldsymbol{D}^{-1} \boldsymbol{A} s_\theta(\boldsymbol{\theta}^*) - \boldsymbol{\theta}^*\right)}_{= \boldsymbol{g}(\boldsymbol{\theta}^*) - \boldsymbol{\theta}^*} = \mathbf{0}. \end{aligned}$$

Thus, the equilibria $\boldsymbol{x}^* = (\boldsymbol{\theta}^*, p^*)$ are the point such that $p^* = \mathbf{1}^\top \boldsymbol{E}(\boldsymbol{\theta}^*)/\gamma$ and $\boldsymbol{\theta}^*$ verify

$$\begin{aligned} &\left(\mathbf{I} - \operatorname{diag}(\boldsymbol{\theta}^*)\right)\left(\mathbf{I} + \operatorname{diag}(\boldsymbol{\theta}^*)\right)\left(\boldsymbol{g}(\boldsymbol{\theta}^*) - \boldsymbol{\theta}^*\right) = \mathbf{0} \\ \Leftrightarrow &\forall i \in \mathcal{V},\ e_i^\top \left(\mathbf{I} - \operatorname{diag}(\boldsymbol{\theta}^*)\right)\left(\mathbf{I} + \operatorname{diag}(\boldsymbol{\theta}^*)\right)\left(\boldsymbol{g}(\boldsymbol{\theta}^*) - \boldsymbol{\theta}^*\right) = 0 \\ \Leftrightarrow &\forall i \in \mathcal{V},\ \left(1 - \theta_i\right)\left(1 + \theta_i\right) e_i^\top \left(\boldsymbol{g}(\boldsymbol{\theta}^*) - \boldsymbol{\theta}^*\right) = 0 \\ \Leftrightarrow &\forall i \in \mathcal{V},\ \left(1 - \theta_i\right)\left(1 + \theta_i\right)\left(e_i^\top \boldsymbol{g}(\boldsymbol{\theta}) - \theta_i\right) = 0, \end{aligned}$$

which is equivalent to $\boldsymbol{\theta}^* \in \mathcal{F}$. □

Proposition 1 provides a condition that must be satisfied by equilibria of the system (3) and, by extension, the set of all equilibria of the dynamics (3).

Remark 2. It is noteworthy that $\operatorname{Fix}(\boldsymbol{g}) \subset \mathcal{F}$. Indeed, to ensure the existence of a nontrivial equilibrium (neither $-\mathbf{1}$ nor $\mathbf{1}$), it is sufficient to ensure that $\operatorname{Fix}(\boldsymbol{g}) \neq \emptyset$.

The following lemma ensures the existence of fixed points for $\boldsymbol{g}$ under signal continuity, thereby establishing the existence of a nontrivial equilibrium for the dynamics (3).

Lemma 2. *Let s_p and s_θ be continuous functions. Then, the function $\boldsymbol{g} : \boldsymbol{\Theta} \to \boldsymbol{\Theta}$ from (4) has at least one fixed point on $\boldsymbol{\Theta}$.*

Let us note that $\boldsymbol{\Theta}$ is convex and compact (recall that $\boldsymbol{\Theta} = [-1, 1]^N$) and $\boldsymbol{g} : \boldsymbol{\Theta} \to \boldsymbol{\Theta}$ is continuous. Then, this lemma is a direct consequence of Brouwer's fixed point theorem [23].

Keeping in mind that a classical solution that received a lot of attention in opinion dynamics is the consensus or synchronization of opinions, it is natural to consider this particular situation in the sequel.

Let us note $\tilde{s}_p(\theta) : \Theta \to \Theta$, the function such that $\tilde{s}_p(\theta) = s_p(\bar{p} - N E(\theta)/\gamma)$.

Lemma 3. *Let $\theta^* \in \operatorname{Fix}(s_\theta) \cap \operatorname{Fix}(\tilde{s}_p)$. Then, the vector $\boldsymbol{x}^* = (\theta^*, \mathbf{1}^\top \boldsymbol{E}(\theta^*)/\gamma)$ where $\theta^* = \theta^* \mathbf{1}$ is a nontrivial equilibrium of (3). Moreover, if s_p is continuous, then $\left|\operatorname{Fix}(s_\theta) \cap \operatorname{Fix}(\tilde{s}_p)\right| \leq 1$.*

Proof. By definition, $E : \Theta \to \mathbb{R}$ and $s_p : \mathbb{R} \to \Theta$ are non-decreasing in their argument, yielding that $_p(\theta) = s_p(\bar{p} - N E(\theta)/\gamma)$ is a non-increasing function in θ. Since $\tilde{s}_p : \Theta \to \Theta$ is decreasing, it has at most one fixed point. Indeed by contradiction, assuming that $x, y \in \operatorname{Fix}(\tilde{s}_p)$ such that $x < y$, then one has $x = \tilde{s}_p(x) > \tilde{s}_p(y) = y$ which is a

contradiction. Moreover, adding the assumption that $\tilde{s}_p$ is continuous and using Brouwer's fixed-point theorem [23] yields the existence of a fixed point. Thus, the fixed point of $\tilde{s}_p$ is unique under continuity assumption and one has $\left|\text{Fix}\left(s_\theta\right) \cap \text{Fix}\left(\tilde{s}_p\right)\right| \leq \left|\text{Fix}\left(\tilde{s}_p\right)\right| = 1$.

Assuming $\text{Fix}\left(s_\theta\right) \cap \text{Fix}\left(\tilde{s}_p\right)$ being non-empty, let $\theta \in \text{Fix}\left(s_\theta\right) \cap \text{Fix}\left(\tilde{s}_p\right)$ and let $\boldsymbol{\theta} = \theta\mathbf{1}$. From Proposition 1, for $\boldsymbol{\theta}$ to be an equilibrium, it needs to verify (5). If $\theta \in \{-1, 1\}$ this condition is immediately met. But it is noteworthy that with the Standing Assumption 1 such points cannot be fixed point of $\tilde{s}_p$ and thus $-1, 1 \notin \text{Fix}\left(s_\theta\right) \cap \text{Fix}\left(\tilde{s}_p\right)$. If instead, $\theta \in (-1, 1)$, $\boldsymbol{\theta}$ has to be a fixed point of $\boldsymbol{g}$ and rewriting $\boldsymbol{g}(\boldsymbol{\theta}) - \boldsymbol{\theta}$ yields

$$\begin{aligned}
&\boldsymbol{g}(\boldsymbol{\theta}) - \boldsymbol{\theta} = \beta\left(\tilde{s}_p(\boldsymbol{\theta}) - \boldsymbol{\theta}\right) + (1-\beta)\left(\boldsymbol{D}^{-1}\boldsymbol{A}\boldsymbol{s}_\theta(\boldsymbol{\theta}) - \theta\mathbf{1}\right)\\
&= \beta(\theta - \theta)\mathbf{1} + (1-\beta)\theta\boldsymbol{D}^{-1}(\boldsymbol{A}\mathbf{1} - \boldsymbol{D}\mathbf{1})\\
&= -(1-\beta)\theta\boldsymbol{D}^{-1}\boldsymbol{L}\mathbf{1}.
\end{aligned}$$

But the all-ones vector $\mathbf{1}$ is an eigenvector of the Laplacian matrix with eigenvalue 0, one has $-(1-\beta)\theta\boldsymbol{D}^{-1}\boldsymbol{L}\mathbf{1} = \mathbf{0}$. □

Keeping in mind the particular case where the signals of opinions between neighbors are the opinions themselves, we can formulate the following remark.

Remark 3. If $s_\theta = \text{Id}$, Lemma 3 states that $\theta^* \in \text{Fix}\left(\tilde{s}_p\right)$ is a sufficient condition for $\boldsymbol{x}^* = (\theta^*\mathbf{1}, N E(\theta^*)/\gamma)$ to be an equilibrium of dynamics (3).

It is then natural to ask if $\theta \in \text{Fix}\left(s_\theta\right) \cap \text{Fix}\left(\tilde{s}_p\right)$ is a necessary condition for consensus to be an equilibrium of dynamics (3). Let us note, the scalar version of $\boldsymbol{g}$ as $g : \Theta \to \Theta$ such that $g = \beta\tilde{s}_p + (1-\beta)s_\theta$. The following proposition reply to this question by proving that, indeed, the consensus is only attained at a fixed point of g.

Proposition 2. *Let $\boldsymbol{x}^* = \left(\theta^*, \mathbf{1}^\top \boldsymbol{E}(\theta^*)/\gamma\right)$ be an equilibrium of (3) such that $\exists\theta^* \in (-1, 1)$ and $\boldsymbol{\theta}^* = \theta^*\mathbf{1}$. Then $\theta^* \in \text{Fix}(g)$.*

Proof. We have the following equivalences

$$\begin{aligned}
&\boldsymbol{g}\left(\boldsymbol{\theta}^*\right) = \boldsymbol{\theta}^*\\
&\Leftrightarrow \beta s_p\left(\bar{p} - \frac{\mathbf{1}^\top \boldsymbol{E}(\boldsymbol{\theta}^*)}{\gamma}\right)\mathbf{1} + (1-\beta)\boldsymbol{D}^{-1}\boldsymbol{A}\boldsymbol{s}_\theta\left(\boldsymbol{\theta}^*\right) = \boldsymbol{\theta}^*\\
&\Leftrightarrow \beta s_p\left(\bar{p} - \frac{\mathbf{1}^\top \boldsymbol{E}(\boldsymbol{\theta}^*)}{\gamma}\right)\mathbf{1} + (1-\beta)\boldsymbol{s}_\theta\left(\boldsymbol{\theta}^*\right) +\\
&\qquad (1-\beta)\left(\boldsymbol{D}^{-1}\boldsymbol{A}\boldsymbol{s}_\theta\left(\boldsymbol{\theta}^*\right) - \boldsymbol{s}_\theta\left(\boldsymbol{\theta}^*\right)\right) = \boldsymbol{\theta}^*\\
&\Leftrightarrow \beta s_p\left(\bar{p} - \frac{N E(\boldsymbol{\theta}^*)}{\gamma}\right)\mathbf{1} + (1-\beta)s_\theta\left(\boldsymbol{\theta}^*\right)\mathbf{1}\\
&\qquad -(1-\beta)s_\theta\left(\boldsymbol{\theta}^*\right)\boldsymbol{D}^{-1}\boldsymbol{L}\mathbf{1} = \boldsymbol{\theta}^*\mathbf{1}\\
&\Leftrightarrow \beta s_p\left(\bar{p} - \frac{N E(\boldsymbol{\theta}^*)}{\gamma}\right) + (1-\beta)s_\theta\left(\boldsymbol{\theta}^*\right) = \boldsymbol{\theta}^*\\
&\Leftrightarrow g\left(\boldsymbol{\theta}^*\right) = \boldsymbol{\theta}^* \Leftrightarrow \boldsymbol{\theta}^* \in \text{Fix}\left(\beta\tilde{s}_p + (1-\beta)s_\theta\right).
\end{aligned}$$

□

Now, if $s_\theta = \text{Id}$, combining Remark 3 and Proposition 2 yields that consensus must be at fixed points of $\tilde{s}_p$, i.e. the vector $\boldsymbol{x}^* = (\theta^*\mathbf{1}, N E(\theta^*)/\gamma)$ is a equilibrium of dynamics (3) if and only if $\theta^* \in \text{Fix}\left(\tilde{s}_p\right)$. The next Proposition goes further by stating that dynamics (3), in case of linear signaling dynamics over a connected graph, has a unique equilibrium which is a consensus.

Proposition 3. *Let $\mathcal{G}$ be a strongly connected graph and $s_\theta = \text{Id}$. Then dynamics (3) has a unique equilibrium without extreme opinions given by $\boldsymbol{x}^* = (\theta^*\mathbf{1}, N E(\theta^*)/\gamma)$ such that $\theta^* \in \text{Fix}\left(\tilde{s}_p\right)$.*

Proof. As stated above, combining Lemma 3 and Proposition 2, we know that $\boldsymbol{x}^*$ is one equilibrium of (3). To prove it is unique, let assume that $\boldsymbol{\theta}^*$ is a fixed point of $\boldsymbol{g}$, then

$$\begin{aligned}
\boldsymbol{g}\left(\boldsymbol{\theta}^*\right) = \boldsymbol{\theta}^* &\Leftrightarrow \beta s_p\left(\bar{p} - \frac{\mathbf{1}^\top \boldsymbol{E}(\boldsymbol{\theta}^*)}{\gamma}\right)\mathbf{1} + (1-\beta)\boldsymbol{D}^{-1}\boldsymbol{A}\boldsymbol{\theta}^* = \boldsymbol{\theta}^*\\
&\Leftrightarrow s_p\left(\bar{p} - \frac{\mathbf{1}^\top \boldsymbol{E}(\boldsymbol{\theta}^*)}{\gamma}\right)\mathbf{1} - \frac{1-\beta}{\beta}\boldsymbol{D}^{-1}\boldsymbol{L}\boldsymbol{\theta}^* = \boldsymbol{\theta}^*.
\end{aligned}$$

In [24], it is shown that for any strongly connected graph, the associated Laplacian matrix $\boldsymbol{L}$ has eigenvalue 0 with multiplicity 1. Taking $\boldsymbol{v}$ the left eigenvector of $\boldsymbol{L}$ associated with the eigenvalue 0. Multiplying by $\boldsymbol{v}^\top\boldsymbol{D}$, on the left side the equation above yields,

$$\begin{aligned}
&\boldsymbol{v}^\top\boldsymbol{D}\left(s_p\left(\bar{p} - \frac{\mathbf{1}^\top \boldsymbol{E}(\boldsymbol{\theta}^*)}{\gamma}\right)\mathbf{1} - \frac{1-\beta}{\beta}\boldsymbol{D}^{-1}\boldsymbol{L}\boldsymbol{\theta}^*\right) = \boldsymbol{v}^\top\boldsymbol{D}\boldsymbol{\theta}^*\\
&\Leftrightarrow s_p\left(\bar{p} - \frac{\mathbf{1}^\top \boldsymbol{E}(\boldsymbol{\theta}^*)}{\gamma}\right)\boldsymbol{v}^\top\boldsymbol{D}\mathbf{1} - \frac{1-\beta}{\beta}\boldsymbol{v}^\top\boldsymbol{D}\boldsymbol{D}^{-1}\boldsymbol{L}\boldsymbol{\theta}^* = \boldsymbol{v}^\top\boldsymbol{D}\boldsymbol{\theta}^*\\
&\Leftrightarrow s_p\left(\bar{p} - \frac{\mathbf{1}^\top \boldsymbol{E}(\boldsymbol{\theta}^*)}{\gamma}\right) = \frac{\boldsymbol{v}^\top\boldsymbol{D}\boldsymbol{\theta}^*}{\boldsymbol{v}^\top\boldsymbol{D}\mathbf{1}}.
\end{aligned}$$

This allows us to rewrite,

$$\begin{aligned}
\boldsymbol{g}\left(\boldsymbol{\theta}^*\right) = \boldsymbol{\theta}^* &\Leftrightarrow \beta\frac{\boldsymbol{v}^\top\boldsymbol{D}\boldsymbol{\theta}^*}{\boldsymbol{v}^\top\boldsymbol{D}\mathbf{1}}\mathbf{1} + (1-\beta)\boldsymbol{D}^{-1}\boldsymbol{A}\boldsymbol{\theta}^* = \boldsymbol{\theta}^*\\
&\Leftrightarrow \beta\frac{\mathbf{1}\boldsymbol{v}^\top\boldsymbol{D}}{\boldsymbol{v}^\top\boldsymbol{D}\mathbf{1}}\boldsymbol{\theta}^* + (1-\beta)\boldsymbol{D}^{-1}\boldsymbol{A}\boldsymbol{\theta}^* = \boldsymbol{\theta}^*\\
&\Leftrightarrow \left[\mathbf{I} - \left(\beta\frac{\mathbf{1}\boldsymbol{v}^\top\boldsymbol{D}}{\boldsymbol{v}^\top\boldsymbol{D}\mathbf{1}} + (1-\beta)\boldsymbol{D}^{-1}\boldsymbol{A}\right)\right]\boldsymbol{\theta}^* = \mathbf{0}.
\end{aligned}$$

This linear map can now be seen as the Laplacian matrix of a new strongly connected, positively weighted graph. Indeed, the matrix $\mathbf{1}\boldsymbol{v}^\top\boldsymbol{D}/\boldsymbol{v}^\top\boldsymbol{D}\mathbf{1}$ can be interpreted as the adjacency matrix of a uniformly positively weighted all-to-all graph, with self-loops for each agent. Moreover, performing a convex combination of the adjacency matrix of this new graph with the one of the strongly connected, positively weighted influence graph $\boldsymbol{D}^{-1}\boldsymbol{A}$ results in an new adjacency matrix of a strongly connected graph. Finally, the degree matrix of this new graph is the identity matrix $\mathbf{I}$ since, $\forall i \in \mathcal{V}$, one has

$$e_i^\top\left(\beta\frac{\mathbf{1}\boldsymbol{v}^\top\boldsymbol{D}}{\boldsymbol{v}^\top\boldsymbol{D}\mathbf{1}} + (1-\beta)\boldsymbol{D}^{-1}\boldsymbol{A}\right) = \beta + 1 - \beta = 1.$$

Since the resulting mapping is a Laplacian matrix of a strongly connected graph, it is well known that its kernel is reduced to $\{\alpha\mathbf{1} \mid \alpha \in \mathbb{R}\}$. Therefore, the only fixed point of $\boldsymbol{g}$ is $\boldsymbol{\theta}^* \in \{\alpha\mathbf{1} \mid \alpha \in \mathbb{R}\} \cap \text{Fix}(\tilde{s}_p)$, i.e., $\boldsymbol{\theta}^* = \theta^*\mathbf{1}$ such that $\theta^* \in \text{Fix}(\tilde{s}_p)$. □

We note that Proposition 3 highlights a situation in which all the opinions reach a common value. It basically says that if each individual has access to the exact opinions of its neighbors in a strongly connected graph, they will reach a consensus. Moreover, the consensus value is determined by the external signal coupled with the opinion dynamics.

From now on, we denote by $g_i(\boldsymbol{\theta}) := e_i^\top\boldsymbol{g}(\boldsymbol{\theta})$ for any $i \in \mathcal{V}$. We note that equilibrium may depend not only on the signal function but also on the topology of the graph. Particularly, when symmetry of observation between neighbors arises, we can formulate the following result.

Proposition 4. *Let $\boldsymbol{x}^* = \left(\boldsymbol{\theta}^*, p^*\right)$ be a nontrivial equilibrium point of the dynamic (3) and let $i, j \in \mathcal{V}$ such that $i \neq j$. If "$\mathcal{N}_i = \mathcal{N}_j$" or "$\mathcal{N}_j = \mathcal{N}_i \cup \{i\}$ and $\mathcal{N}_i = \mathcal{N}_j \cup \{j\}$", then we have $\theta_i^* = \theta_j^*$.*

Proof. If $\boldsymbol{x}^*$ is a nontrivial equilibrium of (3), one has $\boldsymbol{g}(\boldsymbol{\theta}^*) = \boldsymbol{\theta}^*$ yielding, for i and $j \in \mathcal{V}$,

$$\begin{cases} g_i(\boldsymbol{\theta}^*) - \theta_i^* = 0\\ g_j(\boldsymbol{\theta}^*) - \theta_j^* = 0 \end{cases} \Leftrightarrow \begin{cases} g_i(\boldsymbol{\theta}^*) - \theta_i^* = 0\\ g_i(\boldsymbol{\theta}^*) - \theta_i^* = g_j(\boldsymbol{\theta}^*) - \theta_j^*. \end{cases}$$

The second equation in the system above is rewritten as:

$$\frac{(1-\beta)}{n}\left(e_j^\top\boldsymbol{A} - e_i^\top\boldsymbol{A}\right)s_\theta\left(\boldsymbol{\theta}^*\right) = \theta_j^* - \theta_i^*,$$

where $n = n_i = n_j$ the numbers of neighbors of i and j.

Let us note that $\forall k \in \mathcal{V}$, $e_k^\top\boldsymbol{A}$ is the vector with the component related to the neighbors of k equal 1 and all the others equal 0. If

$\mathcal{N}_i = \mathcal{N}_j$, we have $e_i^\top \boldsymbol{A} = e_j^\top \boldsymbol{A}$ and the result became obvious. If i and j are neighbors, i.e. $j \in \mathcal{N}_i$ and $i \in \mathcal{N}_j$, one has $\mathcal{N}_i \neq \mathcal{N}_j$ but $\mathcal{N}_i \cap \mathcal{N}_j = \mathcal{N}_i \setminus \{j\} = \mathcal{N}_j \setminus \{i\}$. In this case, $e_i^\top \boldsymbol{A} - e_j^\top = e_j^\top \boldsymbol{A} - e_i^\top$. We proceed by contradiction and assume that $\theta_i^* \neq \theta_j^*$, without loss of generality, we can assume that $\theta_i < \theta_j$. Now, the equation becomes

$$\frac{(1-\beta)}{n}\left(e_i^\top - e_j^\top\right) \boldsymbol{s}_\theta\left(\boldsymbol{\theta}^*\right) = \theta_j^* - \theta_i^*$$
$$\Leftrightarrow \frac{(1-\beta)}{n}\left(s_\theta\left(\theta_i^*\right) - s_\theta\left(\theta_j^*\right)\right) = \theta_j^* - \theta_i^*.$$

Since s_θ is monotonically increasing we obtain a contradiction. Indeed, the left-hand side is non-positive while the right-hand side is strictly positive. This is a contradiction, which implies that we must have $\theta_i^* = \theta_j^*$. □

Proposition 4 says that, at equilibrium, and for any monotonous increasing signaling function, two different agents with identical observation will have the same opinions. A direct consequence of this proposition is that if the graph is all-to-all, then the nontrivial equilibrium point corresponds to consensus.

3.2. Stability analysis of equilibria

In the following, we will assume that s_θ, s_p, and E are differentiable functions. From Proposition 1, the Jacobian of $\mathbf{F}$ is given by

$$\mathbf{J}(\theta, p) = \begin{bmatrix} \dfrac{\partial \boldsymbol{u}(\boldsymbol{\theta}, p)}{\partial \boldsymbol{\theta}} & -\beta s_p'\left(\bar{p} - p\right)\left(\mathbf{I} - \operatorname{diag}\left(\boldsymbol{\theta}\right)^2\right)\mathbf{1} \\ \nabla \boldsymbol{E}(\boldsymbol{\theta})^\top & 1-\gamma \end{bmatrix}, \tag{6}$$

with

$$\frac{\partial \boldsymbol{u}(\boldsymbol{\theta}, p)}{\partial \boldsymbol{\theta}} = \mathbf{I} - 2\operatorname{diag}\left(\boldsymbol{\theta}\right)\operatorname{diag}\left(\boldsymbol{f}\left(\boldsymbol{\theta}, p\right) - \boldsymbol{\theta}\right) + \left(\mathbf{I} - \operatorname{diag}\left(\boldsymbol{\theta}\right)^2\right)\left[(1-\beta)\,\boldsymbol{D}^{-1}\boldsymbol{A}\operatorname{diag}\left(s_\theta'\left(\boldsymbol{\theta}\right)\right) - \mathbf{I}\right].$$

We have seen earlier that some equilibria of the dynamics can contain extreme values in opinion, i.e. for such equilibrium it exists $i \in \mathcal{V}$, $\theta_i \in \{-1, 1\}$. The following proposition states that such equilibria are unstable.

Theorem 1. *Let $\boldsymbol{x}^* = \left(\boldsymbol{\theta}^*, p^*\right)$ be an equilibrium point of the dynamics (3), $\mathcal{G}$ be a strongly connected graph and s_θ, E and s_p be differentiable functions in $\boldsymbol{\theta}^*$ and $\bar{p} - p^*$, respectively. Then, if it exists $i \in \mathcal{V}$ such that $\theta_i^* \in \{-1, 1\}$, then $\boldsymbol{x}^*$ is an unstable equilibrium.*

Proof. Let $\boldsymbol{x}^* = \left(\boldsymbol{\theta}^*, p^*\right)$ be an equilibrium of (3) such that there exists $i \in \mathcal{V}$ with $\theta_i \in \{-1, 1\}$. By permutation of the index, we can assume without loss of generality that $i = 1$, i.e. $\theta_1^* \in \{-1, 1\}$. Isolating the opinion of agent 1 in the Jacobian matrix given by (6), one can rewrite this Jacobian as the following block matrix

$$\mathbf{J}(\theta, p) = \begin{bmatrix} \mathbf{J}_{11}(\theta, p) & \mathbf{J}_{12}(\theta, p) \\ \mathbf{J}_{21}(\theta, p) & \mathbf{J}_{22}(\theta, p) \end{bmatrix},$$

with $\mathbf{J}_{11} \in \mathbb{R}$ being scalar, $\mathbf{J}_{12}$, $\mathbf{J}_{21}^\top \in \mathbb{R}^N$ being N-vector and $\mathbf{J}_{22} \in \mathbb{R}^{N\times N}$ being a N-square matrix. Noting that $\theta_1^* \in \{-1, 1\}$, one obtains

$$\mathbf{J}_{11}(\boldsymbol{\theta}^*, \frac{\mathbf{1}^\top \boldsymbol{E}\left(\boldsymbol{\theta}^*\right)}{\gamma}) = 1 + 2\theta_1^{*2} - 2\theta_1^* g_1(\boldsymbol{\theta}^*) = 3 - 2\theta_1^* g_1(\boldsymbol{\theta}^*).$$

Moreover, non-diagonal elements of $\partial \boldsymbol{u}(\boldsymbol{\theta}, p)/\partial \boldsymbol{\theta}$ are weighted by $\mathbf{I} - \operatorname{diag}\left(\boldsymbol{\theta}^*\right)^2$ and, since $\theta_1^* \in \{-1, 1\}$, the first row of (6) is null except on its first coordinate yielding,

$$\mathbf{J}_{12}(\boldsymbol{\theta}^*, \frac{\mathbf{1}^\top \boldsymbol{E}\left(\boldsymbol{\theta}^*\right)}{\gamma}) = \begin{bmatrix} 0 & \cdots & 0 \end{bmatrix} = \mathbf{0}_N^\top.$$

By the properties of the determinant of block-triangular matrices, the characteristic polynomial $P_{\mathbf{J}}$ of $\mathbf{J}$ is given by

$$P_{\mathbf{J}}(X) = \det\left(\mathbf{I}_{N+1}X - \mathbf{J}\right) = \det\left(X - \mathbf{J}_{11}\right)\det\left(\mathbf{I}_N X - \mathbf{J}_{22}\right).$$

Then, $\lambda = \mathbf{J}_{11}(\boldsymbol{\theta}^*, \mathbf{1}^\top \boldsymbol{E}\left(\boldsymbol{\theta}^*\right)/\gamma) = 3 - 2\theta_1^* g_1(\boldsymbol{\theta}^*)$ is one of the eigenvalues of the Jacobian matrix (6). Now, either $\boldsymbol{\theta}^* = \pm\mathbf{1}$ or there exists $j \in \mathcal{V}$ such that $\theta_1^* \neq \theta_j^*$. In the first case, one has

$$\left|e_1^\top \boldsymbol{D}^{-1}\boldsymbol{A}\boldsymbol{s}_\theta\left(\boldsymbol{\theta}^*\right)\right| = \left|\frac{1}{n_1}\sum_{j\in\mathcal{N}_1} s_\theta\left(\theta_j^*\right)\right| = 1.$$

Then, for $\boldsymbol{\theta}^* = -\mathbf{1}$,

$$\lambda = 3 + 2\left(\beta\tilde{s}_p(-1) - (1-\beta)\right) = 1 + 2\beta\left(1 + \tilde{s}_p(-1)\right).$$

From Standing Assumption 1, we have $\bar{p} > Ne_{\min}/\gamma$ and since $s_p(p) = 0$ only if $p = 0$, one has $\tilde{s}_p(-1) > 0$. Moreover, noting that $0 < \beta$, yields,

$$\lambda = 1 + 2\beta\left(1 + \tilde{s}_p(-1)\right) > 1.$$

Then, if $\boldsymbol{\theta} = -\mathbf{1}$, at least one eigenvalues of (6) evaluated at $\boldsymbol{x}^*$ is strictly greater than 1. Then, by the linearization principle, $\boldsymbol{x}^*$ is unstable.

If $\boldsymbol{\theta}^* = \mathbf{1}$, similar reasoning apply noting that, since $\bar{p} < Ne_{\max}/\gamma$, one has $\tilde{s}_p(1) = s_p\left(\bar{p} - Ne_{\max}/\gamma\right) < 0$ and then

$$\lambda = 3 - 2\left(\beta\tilde{s}_p(1) + (1-\beta)\right) = 1 + 2\beta\left(1 - \tilde{s}_p(1)\right) > 1.$$

Again, the linearization principle implies that, if $\boldsymbol{\theta}^* = \mathbf{1}$ then $\boldsymbol{x}^*$ is unstable.

If $\boldsymbol{\theta}^*$ is neither $-\mathbf{1}$ nor $\mathbf{1}$, there exists $j \in \mathcal{V}$ such that $\theta_j \neq \theta_1$. Without loss of generality let $j \in \mathcal{N}_1$. Indeed, since the graph is connected and $\boldsymbol{\theta}^* \neq \pm\mathbf{1}$, there exists at least one $i \in \mathcal{V}$ with $\theta_i^* \in \{-1, 1\}$ such that there $\exists j \in \mathcal{N}_i$ verifying $\theta_j^* \neq \theta_i^*$. By permutation of the labeling, one can assume there $\exists j \in \mathcal{N}_1$ such that $\theta_j^* \neq \theta_1^*$. Now, one has,

$$\left|e_1^\top \boldsymbol{D}^{-1}\boldsymbol{A}\boldsymbol{s}_\theta\left(\boldsymbol{\theta}^*\right)\right| = \left|\frac{1}{n_1}\sum_{j\in\mathcal{N}_1} s_\theta\left(\theta_j^*\right)\right| < 1,$$

and since $0 < \beta < 1$, we have

$$\left|g_1\left(\boldsymbol{\theta}^*\right)\right| = \left|\beta s_p\left(\bar{p} - \frac{\mathbf{1}^\top \boldsymbol{E}\left(\boldsymbol{\theta}^*\right)}{\gamma}\right) + (1-\beta)\,e_1^\top \boldsymbol{D}^{-1}\boldsymbol{A}\boldsymbol{s}_\theta\left(\boldsymbol{\theta}^*\right)\right|$$
$$\leq \beta\left|s_p\left(\bar{p} - \frac{\mathbf{1}^\top \boldsymbol{E}\left(\boldsymbol{\theta}^*\right)}{\gamma}\right)\right| + (1-\beta)\left|e_1^\top \boldsymbol{D}^{-1}\boldsymbol{A}\boldsymbol{s}_\theta\left(\boldsymbol{\theta}^*\right)\right| < 1.$$

We have then,

$$\lambda = 3 - 2\theta_1^* g_1\left(\boldsymbol{\theta}^*\right) \geq 3 - 2\left|g_1\left(\boldsymbol{\theta}^*\right)\right| > 1.$$

To conclude, if $\exists i \in \mathcal{V}$ such that $\theta_i^* \in \{-1, 1\}$, the Jacobian evaluated in this point $\mathbf{J}\left(\boldsymbol{\theta}^*, p^*\right)$ has at least one eigenvalue of modulus strictly greater than 1 and thus this equilibrium is unstable. □

The theorem states that, under Standing Assumption 1, for a strongly connected graph, every equilibrium where at least one agent holds an extreme opinion is unstable. This implies that if opinions are allowed to spread freely, perturbing agents with extreme opinions will cause them to doubt and shift towards a less extreme stance. It is important to emphasize that this result requires the assumption of strong connectivity in the graph. For example, if the graph $\mathcal{G}$ has an isolated disconnected agent, an equilibrium in which all the other (connected) agents reach consensus at some non-extreme opinion with the single agent holding the opposing extreme opinion can be locally asymptotically stable.

4. Analysis of the fully synchronized opinions (FSO) case

In this section, we consider that the opinion dynamics evolves much faster than the air pollution state. Consequently, in the sequel the following condition holds true.

Assumption 1. There exists a time-scale separation between the fast variation of θ and the slow variation of p.

Based on Assumption 1 we can use the standard approach in [25] to decouple the overall dynamics into the reduced order model and the boundary layer one. We recall that the boundary layer system evolves on the fast time scale and assumes that the slow variable is constant. In this case, under some regularity condition of signal s_θ, the opinions will converge to a consensus as proven in the next result.

Proposition 5. *Under Assumption 1, let s_θ be a k-Lipschitz function with $k < 1/(1-\beta)$. Then, for any $p \in \mathbb{R}_{\geq 0}$ the function $\theta \mapsto \boldsymbol{f}(\theta, p)$ has a unique fixed point in $\boldsymbol{\Theta}$ given by $\theta^*\mathbf{1}$ with $\theta^* = \mathrm{Fix}\left(\theta \mapsto \beta s_p(\bar{p}-p) + (1-\beta)\, s_\theta(\theta)\right)$.*

Proof. Let s_θ be a k-Lipschitz function, then for any $\theta, \theta' \in \boldsymbol{\Theta}$ and any $p \in \mathbb{R}_{\geq 0}$, one has

$$\left\|\boldsymbol{f}(\boldsymbol{\theta}, p) - \boldsymbol{f}\left(\boldsymbol{\theta}', p\right)\right\|_2 \leq k\,(1-\beta)\left\|\boldsymbol{\theta} - \boldsymbol{\theta}'\right\|_2. \tag{7}$$

Indeed, by expanding the formulation of $\boldsymbol{f}$ in this specific case, one obtains

$$\begin{aligned}
&\left\|\boldsymbol{f}(\boldsymbol{\theta}, p) - \boldsymbol{f}\left(\boldsymbol{\theta}', p\right)\right\|_2 \\
&= \left\|\beta\left(s_p(\bar{p}-p) - s_p(\bar{p}-p)\right)\mathbf{1} + (1-\beta)\,\boldsymbol{D}^{-1}\boldsymbol{A}\left(\boldsymbol{s}_\theta(\boldsymbol{\theta}) - \boldsymbol{s}_\theta\left(\boldsymbol{\theta}'\right)\right)\right\|_2 \\
&= \left\|(1-\beta)\,\boldsymbol{D}^{-1}\boldsymbol{A}\left(\boldsymbol{s}_\theta(\boldsymbol{\theta}) - \boldsymbol{s}_\theta\left(\boldsymbol{\theta}'\right)\right)\right\|_2 \\
&\leq (1-\beta)\left\|\boldsymbol{D}^{-1}\boldsymbol{A}\right\|_{2,2}\left\|\boldsymbol{s}_\theta(\boldsymbol{\theta}) - \boldsymbol{s}_\theta\left(\boldsymbol{\theta}'\right)\right\|_2 \leq (1-\beta)\,k\left\|\boldsymbol{\theta} - \boldsymbol{\theta}'\right\|_2.
\end{aligned}$$

Then, for a constant $p \in \mathbb{R}_{\geq 0}$, $\boldsymbol{f}$ is a contraction with respect to its first variable $\boldsymbol{\theta}$. Therefore, by Banach fixed-point theorem [23], $\boldsymbol{\theta} \mapsto \boldsymbol{f}(\boldsymbol{\theta}, p)$ has a unique fixed point. Let $\boldsymbol{\theta}^*$ be this fixed point, it must verify

$$\begin{aligned}
&\boldsymbol{f}\left(\boldsymbol{\theta}^*, p\right) = \boldsymbol{\theta}^* \Leftrightarrow \beta s_p(\bar{p}-p)\mathbf{1} + (1-\beta)\,\boldsymbol{D}^{-1}\boldsymbol{A}\boldsymbol{s}_\theta\left(\boldsymbol{\theta}^*\right) = \boldsymbol{\theta}^* \\
&\Leftrightarrow \beta s_p(\bar{p}-p)\mathbf{1} + (1-\beta)\,\boldsymbol{s}_\theta\left(\boldsymbol{\theta}^*\right) - \boldsymbol{\theta}^* \\
&\qquad + (1-\beta)\left(\boldsymbol{D}^{-1}\boldsymbol{A}\boldsymbol{s}_\theta\left(\boldsymbol{\theta}^*\right) - \boldsymbol{s}_\theta\left(\boldsymbol{\theta}^*\right)\right) = \mathbf{0} \\
&\Leftrightarrow \beta s_p(\bar{p}-p)\mathbf{1} + (1-\beta)\,\boldsymbol{s}_\theta\left(\boldsymbol{\theta}^*\right) - \boldsymbol{\theta}^* - (1-\beta)\,\boldsymbol{D}^{-1}\boldsymbol{L}\boldsymbol{s}_\theta\left(\boldsymbol{\theta}^*\right) = \mathbf{0}.
\end{aligned}$$

But now, notice that $\tilde{f} : \theta \mapsto \beta s_p(\bar{p}-p) + (1-\beta)\, s_\theta(\theta)$ is also a continuous contraction of Θ. Then, as before, by Banach fixed-point theorem, it has a unique fixed point, say θ^*. Moreover, taking $\boldsymbol{\theta} = \theta^*\mathbf{1}$ verify the above equation since $\boldsymbol{L}\mathbf{1} = \mathbf{0}$. □

Remark 4. The condition $k < 1/(1-\beta)$ imposes a sufficiently high influence of the pollution dynamics on the opinion dynamics compared with the variation speed of the signaling function s_θ.

The time-scale separation and the emergence of consensus shown in Proposition 5 motivate us to focus on the analysis of the reduced order system under the assumption that all opinions in the network are synchronized. From now on, s_θ, s_p and E are differentiable functions and all the agents share the same opinion.

Definition 1. We say that an opinion state $\boldsymbol{\theta}$ is in the FSO regime if and only if $\forall i, j \in \mathcal{V}$, $\theta_i = \theta_j$. i.e. $\boldsymbol{\theta} = \theta\mathbf{1}$ for $\theta \in \Theta$.

The following proposition studies the effect of the dynamics once FSO has been reached.

Proposition 6. *The FSO manifold*

$$M = \left\{\boldsymbol{x} = (\boldsymbol{\theta}, p) \mid \boldsymbol{\theta} = \theta\mathbf{1},\ \textit{for } \theta \in [-1,1],\ p \in \mathbb{R}_{\geq 0}\right\} \subset \mathbb{R}^{N+1},$$

is forward invariant for the dynamics (3). i.e. $\forall \boldsymbol{x} \in M$, $\boldsymbol{F}(\boldsymbol{x}) \in M$.

Proof. Let $\boldsymbol{x} \in M$, by applying the dynamics (3) to $\boldsymbol{x} = (\theta\mathbf{1}, p)$ with $\theta \in [-1,1]$ and $p \in \mathbb{R}_{\geq 0}$, one can write

$$\mathbf{F}(\boldsymbol{x}) = \begin{pmatrix}\boldsymbol{u}(\theta\mathbf{1}, p) \\ \upsilon(\theta\mathbf{1}, p)\end{pmatrix} = \begin{pmatrix}\theta\mathbf{1} + \left(\mathbf{I} - \mathrm{diag}(\theta\mathbf{1})^2\right)(\boldsymbol{f}(\theta\mathbf{1}, p) - \theta\mathbf{1}) \\ (1-\gamma)\,p + \mathbf{1}^\top \boldsymbol{E}(\theta\mathbf{1})\end{pmatrix}.$$

For any, $\theta \in [-1,1]$, $\mathbf{1}^\top \boldsymbol{E}(\theta\mathbf{1}) = N E(\theta)$, and then $(1-\gamma)\,p + N E(\theta) \in \mathbb{R}_{\geq 0}$ since $\gamma < 1$ and $E(\theta) \geq 0$. Moreover, developing

$$\begin{aligned}
&\theta\mathbf{1} + \left(\mathbf{I} - \mathrm{diag}(\theta\mathbf{1})^2\right)(\boldsymbol{f}(\theta\mathbf{1}, p) - \theta\mathbf{1}) \\
&= \theta\mathbf{1} + (1-\theta^2)\mathbf{I}\left(\beta s_p(\bar{p}-p)\mathbf{1} + (1-\beta)\,\boldsymbol{D}^{-1}\boldsymbol{A}\boldsymbol{s}_\theta(\theta\mathbf{1}) - \theta\mathbf{1}\right) \\
&= \theta\mathbf{1} + (1-\theta^2)\mathbf{I}\left(\beta s_p(\bar{p}-p)\mathbf{1} + (1-\beta)\,\boldsymbol{s}_\theta(\theta)\,\boldsymbol{D}^{-1}\boldsymbol{A}\mathbf{1} - \theta\mathbf{1}\right) \\
&= \theta\mathbf{1} + (1-\theta^2)\left(\beta s_p(\bar{p}-p)\mathbf{1} + (1-\beta)\,\boldsymbol{s}_\theta(\theta)\,\mathbf{1} - \theta\mathbf{1}\right) \\
&= \left(\theta + (1-\theta^2)\left(\beta s_p(\bar{p}-p) + (1-\beta)\,s_\theta(\theta) - \theta\right)\right)\mathbf{1} := \theta'\mathbf{1}.
\end{aligned}$$

And since $\theta' \in [-1,1]$, one obtains $\boldsymbol{x} \in M$. □

To simplify the presentation, in the FSO regime, we will denote $\theta(k)$ and the common opinion. In other words, we omit the agent index when referring to its opinion or emission.

Under the assumption that $\boldsymbol{\theta}$ is in FSO regime, the opinion dynamics of any agent coupled with the environment in (3) rewrites as

$$\boldsymbol{x}(k+1) = \mathbf{F}(\boldsymbol{x}(k)) = \begin{pmatrix}u(\theta(k), p(k)) \\ \upsilon(\theta(k), p(k))\end{pmatrix}, \tag{8}$$

with the scalar function

$$u(\theta, p) = \theta + \left(1-\theta^2\right)(f(\theta, p) - \theta),$$

where

$$f(\theta, p) = \beta s_p(\bar{p}-p) + (1-\beta)\,s_\theta(\theta).$$

Now, the Jacobian of the dynamics becomes:

$$\mathbf{J}(\theta, p) = \begin{bmatrix}\dfrac{\partial u}{\partial \theta}(\theta, p) & -\beta\left(1-\theta^2\right)s_p'(\bar{p}-p) \\ E'(\theta) & 1-\gamma\end{bmatrix}$$

with

$$\frac{\partial u}{\partial \theta}(\theta, p) = 1 - 2\theta\,(f(\theta, p) - \theta) + \left(1-\theta^2\right)\left((1-\beta)\,s_\theta'(\theta) - 1\right).$$

The dynamics preserves the properties established in the general case. For instance, the equilibrium $\boldsymbol{x}^* = (\theta^*, p^*)$ with $\theta^* \in \{-1, 1\}$ is unstable by Theorem 1. This justifies our focus on the stability analysis of equilibrium of the form $\boldsymbol{x}^* = (\theta^*, N E(\theta^*)/\gamma)$, with $\theta^* \in \mathrm{Fix}(g)$, (recall that $g = \beta\tilde{s}_p + (1-\beta)\,s_\theta$). In FSO, the Jacobian slightly changes due to the term $\partial u/\partial\theta$ that becomes:

$$\frac{\partial u}{\partial \theta}(\theta, p) = 1 + \left(1-\theta^2\right)\left((1-\beta)\,s_\theta'(\theta) - 1\right).$$

Now, the characteristic polynomial of $\mathbf{J}$ is given by:

$$\begin{aligned}
P(X) = X^2 &- \left(2 + \left(1-\theta^2\right)\left((1-\beta)\,s_\theta'(\theta) - 1\right) - \gamma\right)X \\
&+ \left(1 + \left(1-\theta^2\right)\left((1-\beta)\,s_\theta'(\theta) - 1\right)\right)(1-\gamma) \\
&+ \beta\left(1-\theta^2\right)E'(\theta)s_p'\left(\bar{p} - \frac{N E(\theta)}{\gamma}\right).
\end{aligned} \tag{9}$$

And its discriminant is given by:

$$\begin{aligned}
\Delta_P = &\left(\left(1-\theta^2\right)\left((1-\beta)\,s_\theta'(\theta) - 1\right) + \gamma\right)^2 \\
&- 4\beta\left(1-\theta^2\right)E'(\theta)s_p'\left(\bar{p} - \frac{N E(\theta)}{\gamma}\right).
\end{aligned}$$

To simplify the stability analysis of equilibria, let us state the following intermediate lemma that provides conditions to ensure that roots of a polynomial are of modulus less than 1.

Lemma 4. *Let $P(X) = X^2 + bX + c$ be a second-order polynomial with $b, c \in \mathbb{R}$ such that its discriminant $\Delta_P = b^2 - 4c \geq 0$ and denote its roots $\lambda_1 = \left(-b - \sqrt{\Delta_P}\right)/2$ and $\lambda_2 = \left(-b + \sqrt{\Delta_P}\right)/2$. Then, $|\lambda_1| < 1$ and $|\lambda_2| < 1$ if and only if $|b| < 1 + c$ with $b \in (-2, 2)$.*

Proof. Note that $|\lambda_1| < 1$ and $|\lambda_2| < 1$ is equivalent with

$$-1 < \lambda_1 \leq \lambda_2 < 1 \Leftrightarrow -2 + b < -\sqrt{\Delta_P} \leq \sqrt{\Delta_P} < 2 + b$$

yielding $0 \leq \sqrt{\Delta_P} < 2 - |b|$ which requires that $b \in (-2, 2)$. Moreover

$$\begin{aligned}
\sqrt{\Delta_P} < 2 - |b| &\Leftrightarrow b^2 - 4c < 4 - 4|b| + b^2 \\
&\Leftrightarrow |b| < 1 + c
\end{aligned}$$

which concludes the proof. □

The following proposition characterizes the stability of the equilibrium point $\theta^* \in \mathrm{Fix}\,(g) \cap (-1,1)$ with respect to the parameters β, γ and the function s_θ and s_p.

Theorem 2. *Let $x^* = (\theta^*, p^*)$ be an equilibrium of the dynamics (8) with $\theta^* \in \mathrm{Fix}\,(g) \cap (-1,1)$. Let P be the characteristic polynomial of $\mathbf{J}$ and note Δ_P its discriminant. Then, x^* is locally exponentially stable if and only if one of the following is verified:*

- *$\Delta_P \geq 0$ and*
$$\max\left(1 - \frac{\gamma + \left(1-\theta^{*2}\right)}{\left(1-\theta^{*2}\right) s'_\theta(\theta^*)}, \frac{\gamma\left(s'_\theta(\theta^*) - 1\right)}{\gamma s'_\theta(\theta^*) + E'(\theta^*) s'_p\left(\bar{p} - \frac{NE(\theta^*)}{\gamma}\right)}\right) < \beta.$$
- *$\Delta_P < 0$ and*
$$\beta\left(E'(\theta^*) s'_p\left(\bar{p} - \frac{NE(\theta^*)}{\gamma}\right) - (1-\gamma) s'_\theta(\theta^*)\right) < \frac{\gamma}{\left(1-\theta^{*2}\right)} - \left(s'_\theta(\theta^*) - 1\right)(1-\gamma).$$

Proof. Notice that in the FSO setup, dynamics (3) reduces to a two-dimensional nonlinear dynamical system for which the study of its Jacobian's eigenvalues is sufficient to characterize the local stability of an equilibrium. Those eigenvalues are the roots of the polynomial (9) i.e., the roots of $P(x) = X^2 + bX + c$ with

$$b = -\left(2 + \left(1-\theta^2\right)\left((1-\beta) s'_\theta(\theta) - 1\right) - \gamma\right)$$

and

$$c = 1 - \gamma + \left(1-\theta^2\right)\left((1-\beta) s'_\theta(\theta) - 1\right)(1-\gamma) + \beta\left(1-\theta^2\right) E'(\theta) s'_p\left(\bar{p} - \frac{NE(\theta)}{\gamma}\right).$$

In the case where, $\Delta_P \geq 0$, we can use Lemma 4. Therefore, $|\lambda_1| < 1$ and $|\lambda_2| < 1$ is equivalent with $b \in (-2,2)$ and $|b| < 1 + c$. First, $b \in (-2,2)$ yields

$$\begin{aligned}
&-2 < b < 2\\
\Leftrightarrow\ &-2 < -\left(2 + \left(1-\theta^2\right)\left((1-\beta) s'_\theta(\theta) - 1\right) - \gamma\right) < 2\\
\Leftrightarrow\ &-4 + \gamma < \left(1-\theta^2\right)\left((1-\beta) s'_\theta(\theta) - 1\right) < \gamma\\
\Leftrightarrow\ &1 + \frac{\gamma - 4}{\left(1-\theta^2\right)} < (1-\beta) s'_\theta(\theta) < 1 + \frac{\gamma}{\left(1-\theta^2\right)}\\
\Leftrightarrow\ &\frac{1}{s'_\theta(\theta)} + \frac{\gamma - 4}{\left(1-\theta^2\right) s'_\theta(\theta)} < (1-\beta) < \frac{1}{s'_\theta(\theta)} + \frac{\gamma}{\left(1-\theta^2\right) s'_\theta(\theta)}\\
\Leftrightarrow\ &1 - \frac{\gamma + \left(1-\theta^2\right)}{\left(1-\theta^2\right) s'_\theta(\theta)} < \beta < 1 + \frac{4 - \gamma - \left(1-\theta^2\right)}{\left(1-\theta^2\right) s'_\theta(\theta)}.
\end{aligned} \tag{10}$$

Let us observe that $0 < 4 - \gamma - \left(1-\theta^2\right), \forall\, \gamma \in (0,1),\ \theta \in \Theta$. This implies that $1 + \left(4 - \gamma - \left(1-\theta^2\right)\right) / \left(1-\theta^2\right) s'_\theta(\theta) > 1$. On the other hand, $\beta \in (0,1)$ which simplifies (10) as $-\left(\gamma + \left(1-\theta^2\right)\right) / \left(1-\theta^2\right) s'_\theta(\theta) < \beta \leq 1$.

It is noteworthy that $2 - \gamma - \left(1-\theta^2\right) > 0,\ \forall\, \gamma \in (0,1),\ \theta \in \Theta$. Thus, $\beta < 1 + \left(2 - \gamma - \left(1-\theta^2\right)\right) / \left(1-\theta^2\right) s'_\theta(\theta)$ is equivalent to

$$\beta\left(1-\theta^2\right) s'_\theta(\theta) < 2 + \left(1-\theta^2\right)\left(s'_\theta(\theta) - 1\right) - \gamma \Leftrightarrow b < 0.$$

Consequently,

$$\begin{aligned}
&|b| < 1 + c \Leftrightarrow -b < 1 + c\\
\Leftrightarrow\ &2 - \gamma + \left(1-\theta^2\right)\left((1-\beta) s'_\theta(\theta) - 1\right) < 2 - \gamma + \left(1-\theta^2\right)\left[\left((1-\beta) s'_\theta(\theta) - 1\right)(1-\gamma) + \beta E'(\theta) s'_p\left(\bar{p} - \frac{NE(\theta)}{\gamma}\right)\right]\\
\Leftrightarrow\ &\gamma\left((1-\beta) s'_\theta(\theta) - 1\right) < \beta E'(\theta) s'_p\left(\bar{p} - \frac{NE(\theta)}{\gamma}\right)\\
\Leftrightarrow\ &\gamma\left(s'_\theta(\theta) - 1\right) < \beta\left(\gamma s'_\theta(\theta) + E'(\theta) s'_p\left(\bar{p} - \frac{NE(\theta)}{\gamma}\right)\right)\\
\Leftrightarrow\ &\frac{\gamma\left(s'_\theta(\theta) - 1\right)}{\gamma s'_\theta(\theta) + E'(\theta) s'_p\left(\bar{p} - \frac{NE(\theta)}{\gamma}\right)} < \beta.
\end{aligned}$$

Combining the inequality above with the first inequality in (10) one gets that if $\Delta_P \geq 0$ then $|\lambda_1| < 1$ and $|\lambda_2| < 1$ is equivalent with

$$\max\left(1 - \frac{\gamma + \left(1-\theta^2\right)}{\left(1-\theta^2\right) s'_\theta(\theta)}, \frac{\gamma\left(s'_\theta(\theta) - 1\right)}{\gamma s'_\theta(\theta) + E'(\theta) s'_p\left(\bar{p} - \frac{NE(\theta)}{\gamma}\right)}\right) < \beta.$$

Let us assume now that $\Delta_P < 0$. The complex roots of P have the same modulus. Let λ_C be the eigenvalue defined by $\lambda_C = \frac{-b + i\sqrt{-\Delta_P}}{2}$. Then $|\lambda_C| = \frac{b^2 - b^2 + 4c}{4} = c$ and the following equivalences hold

$$\begin{aligned}
c < 1 \Leftrightarrow\ &\left(1-\theta^2\right)\left((1-\beta) s'_\theta(\theta) - 1\right)(1-\gamma) + \beta\left(1-\theta^2\right) E'(\theta) s'_p\left(\bar{p} - \frac{NE(\theta)}{\gamma}\right) < \gamma\\
\Leftrightarrow\ &\left((1-\beta) s'_\theta(\theta) - 1\right)(1-\gamma) + \beta E'(\theta) + s'_p\left(\bar{p} - \frac{NE(\theta)}{\gamma}\right) < \frac{\gamma}{\left(1-\theta^2\right)}\\
\Leftrightarrow\ &\left(s'_\theta(\theta) - 1\right)(1-\gamma) + \beta\left(E'(\theta) s'_p\left(\bar{p} - \frac{NE(\theta)}{\gamma}\right) - (1-\gamma) s'_\theta(\theta)\right) < \frac{\gamma}{\left(1-\theta^2\right)}\\
\Leftrightarrow\ &\beta\left(E'(\theta) s'_p\left(\bar{p} - \frac{NE(\theta)}{\gamma}\right) - (1-\gamma) s'_\theta(\theta)\right) < \frac{\gamma}{\left(1-\theta^2\right)} - \left(s'_\theta(\theta) - 1\right)(1-\gamma).
\end{aligned}$$

This concludes the proof. □

It is noteworthy that Lemma 1 states that the set $\mathcal{X} = \Theta \times \left[Ne_{\min}/\gamma, Ne_{\max}/\gamma\right]$ is forward invariant for (3) and then for (8). Thus, when the local stability conditions from Theorem 2 are not satisfied, the trajectory will exhibit either convergence to a limit cycle or a strange attractor.

Let us notice that β characterizes the weight of the air pollution signal in the update of the opinions. When $\beta \to 1$, the opinions will mostly be influenced by the environment, and the peers' influence is negligible. Therefore, when the pollution disappears at high speed (γ small), the dynamics will reach a stable equilibrium. If γ is high enough one obtains a discrete-time prey–predator-like behavior with permanent oscillations.

Let us consider the next two particular cases of the signal s_θ.

4.1. Linear signals

Simpler conditions can be exhibited in the linear signaling OD case and are given in the following corollary.

Corollary 1. *Let $s_\theta(\theta) = \theta$, for all $\theta \in \Theta$ and let $x^* = (\theta^*, p^*)$ be an equilibrium of the dynamics (8) with $\theta^* \in \mathrm{Fix}\,(g) \cap (-1,1)$. Let P be the characteristic polynomial of $\mathbf{J}$ and note Δ_P its discriminant. Then, x^* is stable if and only if either $\Delta_P \geq 0$ or $\Delta_P < 0$ and*

$$\beta\left(E'(\theta^*) s'_p\left(\bar{p} - \frac{NE(\theta^*)}{\gamma}\right) - (1-\gamma)\right) < \frac{\gamma}{\left(1-\theta^{*2}\right)}. \tag{11}$$

The proof is immediate from Theorem 2 by replacing $s'_\theta(\theta) = 1$, for all $\theta \in \Theta$.

These conditions allow us to exhibit the particular point where the topological nature of the equilibrium change and bifurcation may occur. Numerical illustrations of this behavior will be provided in the next section.

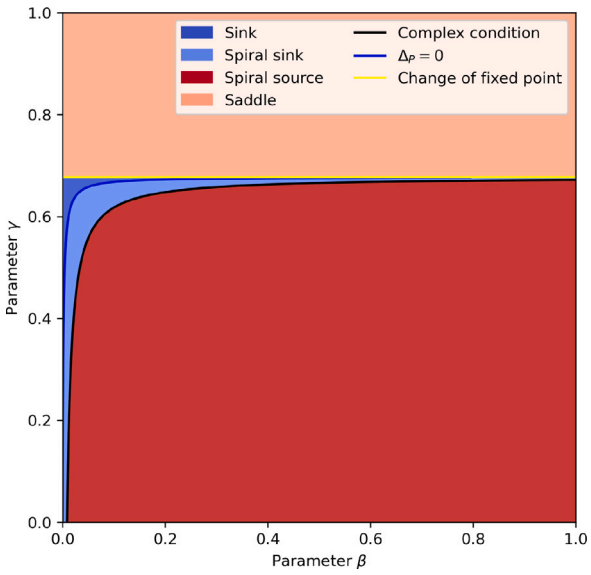


Fig. 1. Topological classification of equilibrium $x^* = (\theta, N E(\theta)/\gamma)$ for the dynamics (8), where $\theta \in \mathrm{Fix}\,(g)$ with $s_\theta(\theta) = \theta$, $s_p = s$, as in (12) with $\delta = 0.05$, $E(\theta) = \theta + 1$ for $0 < \beta, \gamma < 1$, $N = 1$ and $\bar{p} = 2.5$.

4.2. Piece-wise linear signals

In this section, we will look at the particular case where the signal function s_θ and s_p are given by the function

$$s(x) = \begin{cases} -1 & \text{if} \quad x \le -\delta \\ \dfrac{x}{\delta} & \text{if} -\delta \le x \le \delta \\ 1 & \text{if} \quad x \ge \delta. \end{cases} \tag{12}$$

parameterized by $\delta > 0$. This function is piece-wise linear and approximates the sgn function for values of δ close to 0. We will also make the assumption that $E(\theta) = \theta + 1$.

In the particular case of linear OD coupled with the piece-wise linear air pollution signal, i.e. $s_\theta(\theta) = \theta$, $\forall \theta \in \Theta$ and s_p as in (12), we know from Proposition 3 and Lemma 3 that there exists an unique fixed point of the function g. The fixed point of the function g in this case is given by the following expression

$$l(\gamma, \bar{p}, \delta) = \begin{cases} \dfrac{\gamma\bar{p} - 1}{\gamma\delta + 1} & \text{if} \quad \gamma \le \dfrac{2}{\bar{p} - \delta} \\ 1 & \text{otherwise.} \end{cases} \tag{13}$$

The topological nature of the equilibrium associated is illustrated on the β, γ-plane on Fig. 1 for some $\bar{p}$ fixed. We can observe that the nature of the equilibrium changes with respect to the parameters β and γ and is unstable for most of the parameter values. The complex condition black line is given by Eq. (11) and the yellow one from the condition of (13).

In the more general case when both s_θ, s_p are piece-wise linear as in (12), the number of equilibrium points varies with respect to the parameters and accordingly one has different expressions. The following lemma provides conditions under which certain points belong Fix(g). We recall here that $g(\theta) = \beta s(\bar{p} - (\theta + 1)/\gamma) + (1 - \beta)\, s(\theta)$.

Lemma 5. *Let s_θ and s_p be piece-wise linear as in (12). The following statements hold true:*

- *if* $\max\{\theta, \bar{p} - E(\theta)/\gamma\} \le -\delta$, *then* $-1 \in \mathrm{Fix}(g)$.
- *if* $\min\{\theta, \bar{p} - E(\theta)/\gamma\} \ge \delta$, *then* $1 \in \mathrm{Fix}(g)$.
- *if* $\theta \ge \delta$ *and* $\bar{p} - E(\theta)/\gamma \le -\delta$, *then* $-1 + 2\beta \in \mathrm{Fix}(g)$.
- *if* $\theta \le -\delta$ *and* $\bar{p} - E(\theta)/\gamma \ge \delta$, *then* $1 - 2\beta \in \mathrm{Fix}(g)$.
- *if* $|\theta| \ge \delta$ *and* $|\bar{p} - E(\theta)/\gamma| \le \delta$, *then*
$$\frac{sgn(\theta)\,\delta\,(1-\beta) + \beta\,(\bar{p} - 1/\gamma)}{\delta + \beta/\gamma} \in \mathrm{Fix}(g). \tag{14}$$
- *if* $\max\{|\theta|, |\bar{p} - E(\theta)/\gamma|\} \le \delta$, *then*
$$\frac{\beta\,(\bar{p} - 1/\gamma)}{\delta + \beta/\gamma - (1-\beta)} \in \mathrm{Fix}(g). \tag{15}$$
- *if* $|\theta| \le \delta$ *and* $|\bar{p} - E(\theta)/\gamma| \ge \delta$, *then*
$$\frac{sgn(\bar{p} - E(\theta)/\gamma)\,\beta}{1 - (1-\beta)/\delta} \in \mathrm{Fix}(g). \tag{16}$$

The proof of this Lemma is straightforward, every item corresponds to a specific combination between the different possible linear behaviors of the signals s_θ and s_p in (12).

The topological classification of these fixed points can be numerically addressed as in the case of OD with a linear signaling. The numerical analysis is longer and we skip it here since one has to consider all the possible values in Fix(g).

5. Numerical results

This section provides numerical illustrations of the coupled system's behavior. Note that we are numerically analyzing the behavior in the FSO scenario by illustrating the convergence to equilibrium, to a limit cycle, or chaotic trajectories. Additionally, we examine the non-synchronized case, highlighting the formation of clusters and emphasizing again the chaotic behavior. For the sake of simplicity, in the sequel, we take $E(\theta) = \theta + 1$ and denote by s the piece-wise linear approximation of the sign function defined in (12) with $\delta = 0.05$. Moreover, for the rest of the paper, we will also take s_p piece-wise linear, i.e., $s_p = s$.

5.1. Fully synchronized opinion

Let us notice that, synchronization occurs not only when the system reaches a fixed equilibrium as shown in Fig. 2 for two types of signals. The rate of synchronization is influenced by the signal function and the parameter β: lower values of β result in faster synchronization, similar to linear opinion dynamics with exogenous input. Conversely, as β approaches 1, synchronization takes more iterations due to the greater influence of the environment over neighboring interactions, potentially preventing the synchronization.

In the FSO regime, all agents in the system share the same opinion, simplifying the model's dynamics to a two-dimensional system encompassing the common opinion θ and the air pollution state p.

We first examine scenarios with $s_\theta = \mathrm{Id}$ and later, we will illustrate similar behaviors with different interaction signals.

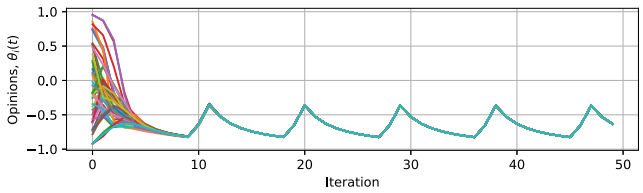
Equilibrium and limit cycle

Under the FSO assumption, the dynamics (8) can exhibit various behaviors depending on the signal and parameters. Notably, the dynamics can converge to an equilibrium or reach a limit cycle.

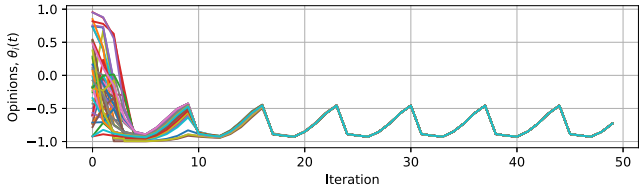
As illustrated in Fig. 3, consistent with Proposition 3, trajectories converge to a unique, attractive in this case, equilibrium $x^* = (\theta^*, E(\theta^*)/\gamma)$, where $\theta^* \in \mathrm{Fix}\,(\tilde{s}_p)$.

Additionally, the dynamics can reach a limit cycle, as shown in Fig. 4, where a 11-period limit cycle appears to stabilize. The length and stability of the limit cycle depend on the parameters β and γ as will be explained in the next section.

The presence of limit cycles indicates a repeating pattern generated by short-term social memory. Population tends to take action when there is a peak of pollution but once the pollution decreases the population considers the problem is solved and returns to standard behavior. This suggests that without interventions to reward the ecologic behavior, the high pollution episodes will persist in time.



(a) s_θ = Id. Synchronization reached in 9 iterations.



(b) $s_\theta = s$, i.e. piece-wise linear. Synchronization reached in 16 iterations.

Fig. 2. Evolution of θ with two signal functions s_θ interacting over a common (randomly generated) strongly connected graph. Parameters: $\beta = 0.3$, $\gamma = 0.5$, $N = 50$, $p(0) = \bar{p} = 25$ and $\theta(0)$ taken as i.i.d. random uniform variables on $[-1, 1]$.

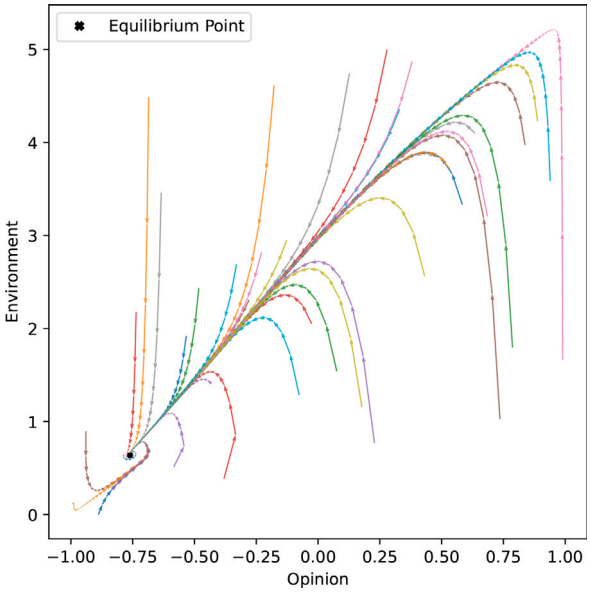


Fig. 3. Phase portrait of dynamics (8) for several trajectories with random initial conditions. Trajectories converge to the unique nontrivial equilibrium. Parameters: $\beta = 0.04$, $\gamma = 0.375$ and $\bar{p} = 0.6$.

Chaos

As evidenced in Fig. 5, the FSO regime can also manifest chaotic behaviors. This figure presents the bifurcation diagram and the associated Lyapunov exponents.

We recall that a dynamical system with Lyapunov exponents that are less than 0 has trajectories that converge to each other. They synchronously reach a stable attractor like a fixed point or a limit cycle. On the other hand, positive Lyapunov exponents indicate chaos or instability, where trajectories diverge exponentially from each other. Under fixed values of γ and $\bar{p}$, a wide range of β values can lead to chaotic dynamics in (8).

Moreover, we can observe that the equilibrium presented in Fig. 3 and the limit cycle of Fig. 4 are both attractive since their associated Lyapunov exponents are negative. It is noteworthy that in Fig. 5, limit cycles present on the bifurcation diagram are always associated with a negative Lyapunov exponent and thus stabilizing.

From an environmental perspective, chaotic behavior is similar to limit cycles. Indeed, although there is no periodic pattern in the evolution of opinions and air pollution, there are permanent oscillations between ecologic actions and high emissions. The main difference lies in the unpredictability of the public response and consequently of the environmental state.

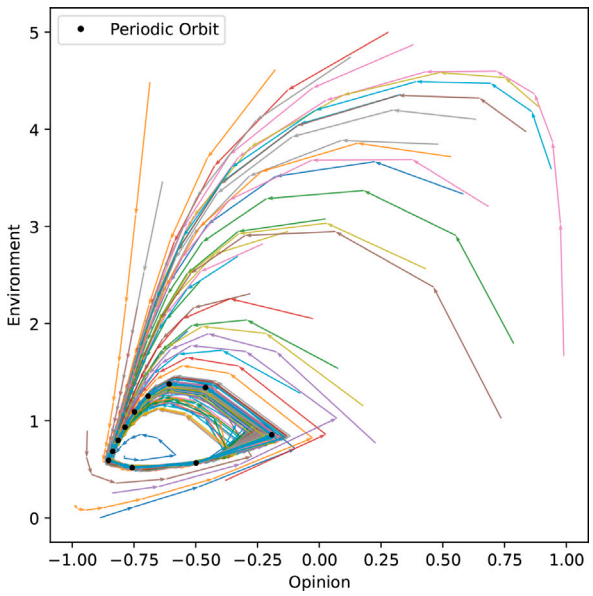


Fig. 4. Phase portrait of dynamics (8) for several trajectories with random initial conditions. Trajectories converge to a 11-period limit cycle. Parameters: $\beta = 0.345$, $\gamma = 0.375$ and $\bar{p} = 0.6$.

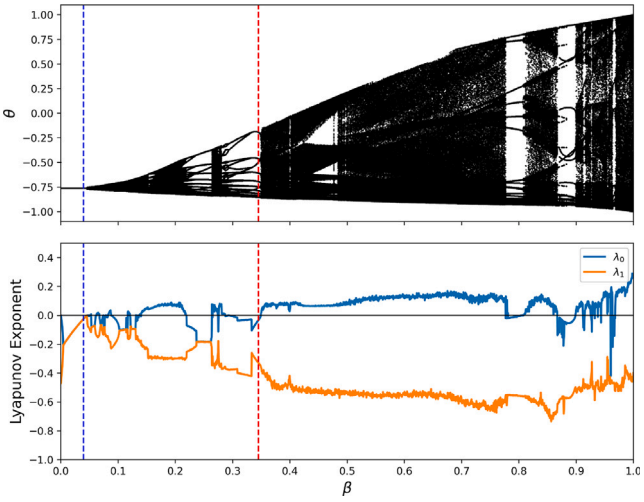
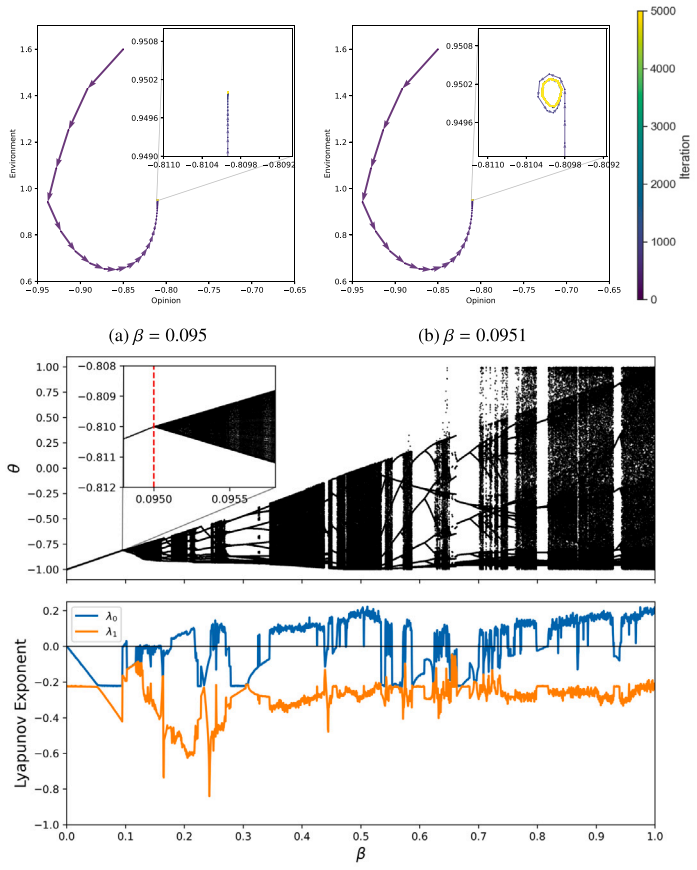


Fig. 5. Bifurcation diagram for $0 < \beta < 1$ of the FSO regime opinion and Lyapunov exponents of the system. The system undergoes different behaviors: convergence to equilibrium, limit cycle, and chaos. The blue line represents the situation of Fig. 3 and the red is the one of Fig. 4. Parameters $\gamma = 0.375$ and $\bar{p} = 0.6$ and initial condition $\theta(0) = -0.5$ and $p(0) = 1.6$. (For interpretation of the references to color in this figure legend, the reader is referred to the web version of this article.)

Other signals

We have noticed through extensive numerical simulations that similar qualitative behaviors are preserved across various signaling functions. This robustness suggests that the fundamental characteristics of the model are independent of the signaling functions. Indeed, we can see in Fig. 6 that trajectories can reach equilibrium for some parameter β like in Fig. 6(a) or strange attractor in Fig. 6(b). Here we can observe the first bifurcation occurring at $\beta = 0.095$ for the associated parameters. This bifurcation, illustrated in Fig. 6(c), presents



(c) Bifurcation diagram of the opinion of the agent and Lyapunov exponents of the system.

Fig. 6. Top: The first 5000 steps of trajectories of (8) before (a) and just after (b) the bifurcation point highlighted (in red) in the bifurcation diagram (c), i.e. $\beta = 0.095$ and $\beta = 0.0951$. A behavioral transition is observed, moving from an equilibrium to a strange attractor. We use $s_\theta = s$ and parameters $\bar{p} = 1$ and $\gamma = 0.2$, with initial condition $\theta(0) = -0.85$ and $p(0) = 1.6$. (c) provides the Bifurcation diagram and Lyapunov exponents for $0 < \beta < 1$. (For interpretation of the references to color in this figure legend, the reader is referred to the web version of this article.)

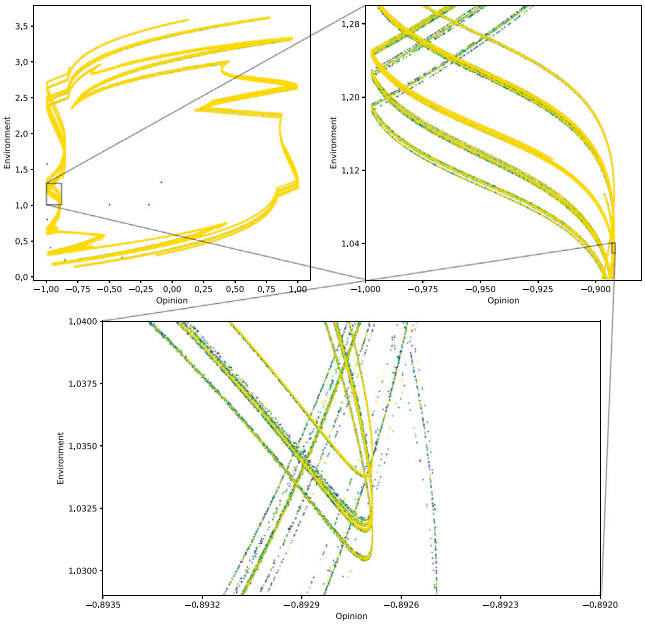


Fig. 7. The trajectory from $k = 0$ to $k = 10,000,000$ with successive zoom for $s_\theta = s$ with parameters: $\beta = 0.916$, $\gamma = 0.5$, and initial condition $p(0) = \bar{p} = 1$ and $\theta(0) = -0.5$. We observe that this trajectory exhibits a fractal pattern.

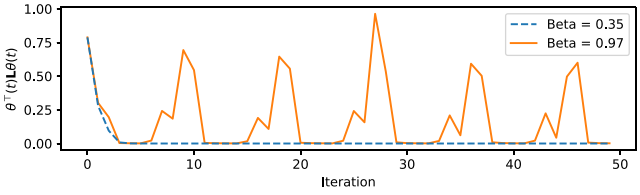


Fig. 8. Chaotic de-synchronization highlighted by $\theta^\top L\theta$ plotted over 50 steps over a randomly generated connected undirected graph for $s_\theta = \mathrm{Id}$. For $\beta = 0.35$, opinions reach FSO over a limit cycle in a few iterations, whereas, for $\beta = 0.97$ consensus is never reached (verified up to 10^6 steps). Parameters: $\gamma = 0.5$, $N = 50$, $p(0) = \bar{p} = 25$ and $\theta(0)$ taken as i.i.d. random uniform variables on $[-1, 1]$.

a transition from convergence towards a stable equilibrium to a strange attractor, which seems to be a Hopf bifurcation.

The presence of a strange attractor, as evidenced by the successive zooms on the phase portrait in Fig. 7, suggests that the system's trajectories are governed by an invariant yet non-periodic underlying structure. During simulations, it has been observed that this attractor folds onto itself as the parameters β and γ change. At lower values of β and γ, as depicted in Fig. 6, the attractor does not exhibit significant folding. However, as β approaches 1 and for $\gamma = 0.5$, the folding phenomenon becomes more pronounced, especially as γ approaches 0.25, as shown in Fig. 7.

While the behavior in the FSO case can be mathematically analyzed, the complexity of the system with multiple interacting agents that are not synchronized hampers a theoretical study.

5.2. Out of sync case

In the following, we numerically analyze the case when the agents do not synchronize. This phenomenon is illustrated in Fig. 8, where agents do not synchronize for a value of β close to 1, even after a large number of iterations. The lack of synchronization and the chaotic behavior are interdependent, and we call this phenomenon chaotic de-synchronization as synchronization occurs in all other regimes.

An examination of the bifurcation diagrams for all agents, as shown in Fig. 9, reveals varying degrees of synchronization. For $\beta < 0.95$, agents tend to synchronize towards FSO; however, for $\beta > 0.95$, agents diverge onto different trajectories. This divergence is further emphasized by the behavior of the associated Lyapunov exponents, which initially evolve in a similar manner but begin to diverge significantly beyond $\beta = 0.95$. This suggests that for values of β close to one, the chaotic behavior intensifies, potentially becoming too strong to permit synchronization.

While the absence of synchronization in chaotic linear signal dynamics is significant, it is not the only scenario in which agents fail to synchronize. Indeed, under certain conditions and signal configurations, clusters of aligned opinions can form, reflecting the graph topology's influence.

Polarized cluster formation

Let us now examine the formation of clusters of opinions under two scenarios, leveraging Proposition 4 to highlight the impact of graph topology, particularly its symmetry, on equilibrium states. We focus on two distinct graph topologies: a block stochastic graph (blocks represented by complete graphs that are connected through few edges) and a sparser 2D-lattice graph. These structures reveal that the formation and behavior of opinion of clusters (stability, polarization, periodicity) significantly depend on the initial conditions and the graph's structure. Specifically, we observe stable polarized clusters in block stochastic graphs as shown in Fig. 10 for the former scenario.

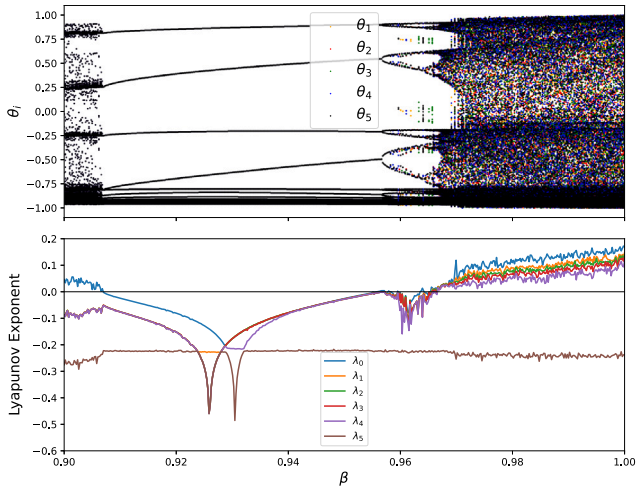
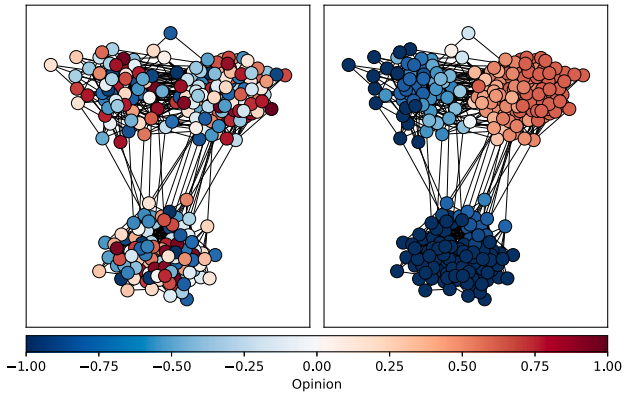
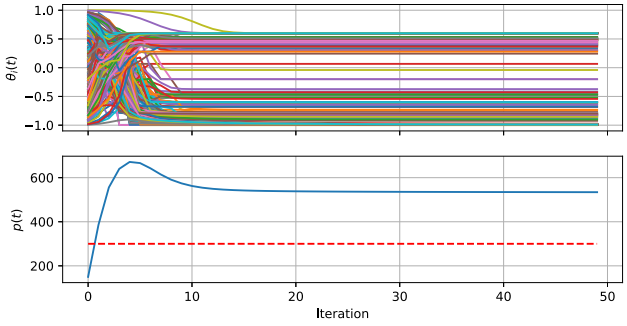


Fig. 9. Bifurcation diagram and Lyapunov exponents for agents 5 over a fully connected graph and the system for $0.9 < \beta < 1$ for $s_\theta = \mathrm{Id}$. For $\beta < 0.95$, agents synchronize whereas for β close to 1, synchronization does not occur anymore. Parameters: $\gamma = 0.2$, $\bar{p} = 4.5$, $p(0) = 30$ and $\boldsymbol{\theta}(0)$ taken as i.i.d. random uniform variables on $[-1, 1]$.



(a) Clustered graph. Left: initial conditions. Right: after 50 iterations.



(b) Evolution of $\boldsymbol{\theta}$ and environment over 50 iterations. Initial conditions: $p(0) = 175$ and $\boldsymbol{\theta}(0)$ taken as i.i.d. random uniform variables on $[-1, 1]$.

Fig. 10. Evolution of the opinion on a randomly generated clustered graph for $s_\theta = s$. We observe that a polarized opinion cluster forms over the graph cluster. Parameters $\beta = 0.2$, $\gamma = 0.44$, $N = 300$ and $\bar{p} = 350$.

On the other hand, Fig. 11 provides insights into the dynamics on a 50×50 square lattice, where initial opinions are randomly distributed and evolve through communication with adjacent nodes. This simulation underscores the formation of resilient clusters that maintain their integrity over numerous iterations, converging to clusters on limit cycles, as can be seen from the opinion trajectory of the nodes in Fig. 11.

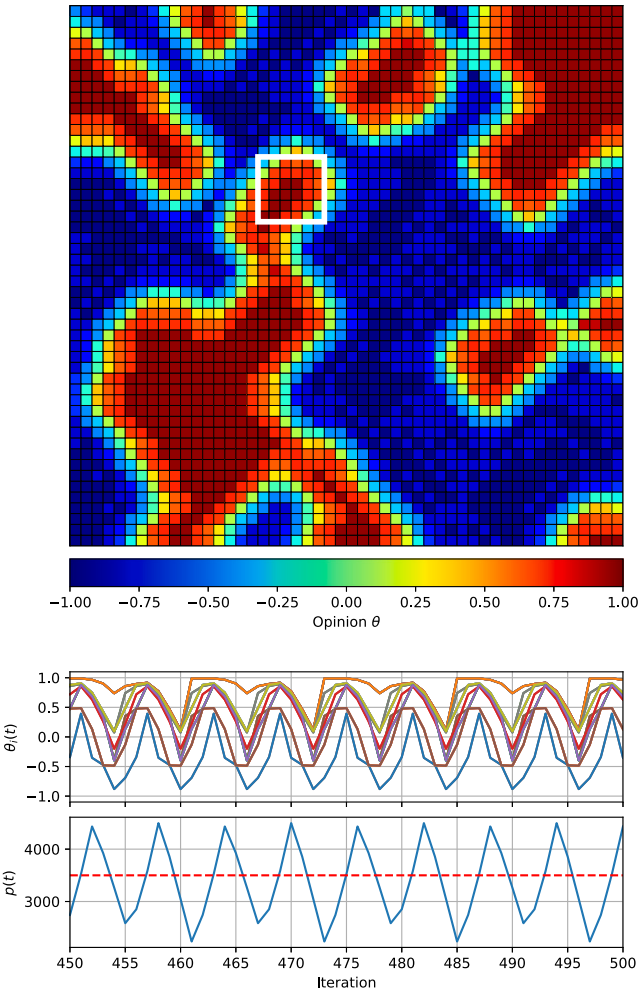


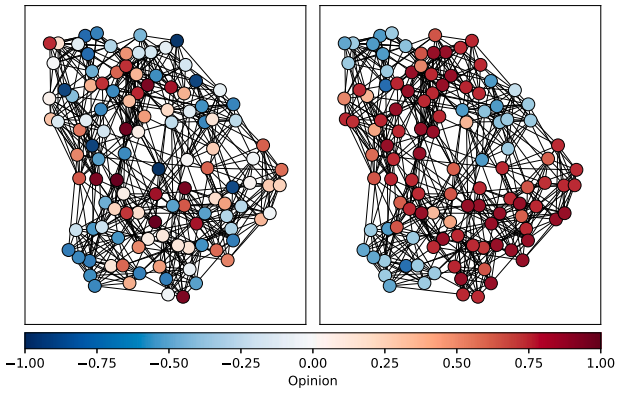
Fig. 11. Visualization of Opinion Dynamics on a 50×50 square Lattice for $s_\theta = s$. The resultant opinions after 500 iterations are represented by each colored square cell. Agents engage in communication with their adjacent cells (above, below, left, and right). The first sub-figure represents opinions over the last 50 iterations of the nodes in the white square. We observe a periodic evolution that maintains the structure of the cluster. The sub-figure below presents the air pollution evolution over the last 50 iterations. Parameters: $\beta = 0.49$, $\gamma = 0.6$, $p(0) = \bar{p} = 3500$, $\boldsymbol{\theta}(0)$ taken as i.i.d. random uniform variables on $[-1, 1]$.

The primary distinction between the two cases is that in the first, the environment reaches an equilibrium and then emits a constant signal, allowing the OD to converge to the stable equilibrium shown in Fig. 10. Conversely, in the second case, the structure of the clusters is preserved but is driven by the air pollution oscillating around $\bar{p}$. The formation of clusters typically occurs in a short amount of time, as depicted in Fig. 10.

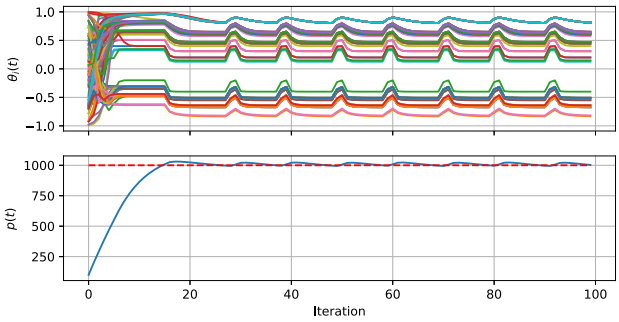
Small-world

This section focuses on numerical simulations conducted on small-world networks, which are analogous to social networks due to their high clustering and short path lengths relative to random networks. Small-world properties are quantified using two metrics: the small-world coefficient σ and the small-world measure ω. A network is considered a small-world if $\sigma > 1$, and its classification between lattice-like ($\omega \approx 1$) and random-like ($\omega \approx -1$) structures is indicated by ω values around zero. Additionally, the diameter of the graph, the longest of all the shortest paths between pairs of nodes, can provide further insight into network topology.

We analyze two graphs from the NetworkX Python library [26] to demonstrate these concepts. The first graph represents the network



(a) Graph of American football clubs, where edges represent games between clubs. The graph contains 115 nodes and is a small-world network with $\sigma = 4.13$ and $\omega = -0.1$. Left: initial conditions. Right: after 100 iterations.



(b) Evolution of $\boldsymbol{\theta}$ and environment over 100 iterations. Initial conditions: $p(0) = 175$ and $\boldsymbol{\theta}(0)$ taken as i.i.d. random uniform variables on $[-1, 1]$.

Fig. 12. Evolution of the opinion on the football club graph for $s_\theta = s$. We observe that polarized opinion clusters form even if the graph does not exhibit obvious clusters. Parameters $\beta = 0.2$, $\gamma = 0.2$, and $\bar{p} = 1000$.

of American football games between Division IA colleges during the regular season of Fall 2000 [27], and the second depicts a portion of a Facebook social network [28]. Our goal here is to demonstrate that the behaviors of dynamics (3) observed in the previous section are scalable and the numerical analysis can be extended to various types of graphs.

Fig. 12 highlights the polarization of opinions in two main clusters despite the absence of clear separation in the initial graph (see Fig. 12(a)). This behavior mirrors that observed in regular grid graphs (see Fig. 11), suggesting that graph regularity is not necessary for cluster formation; rather, it is influenced by parameters β and γ. We remark that the cluster formation is relatively fast and is achieved before the signal p reaches the threshold $\bar{p}$ as shown in Fig. 12(b).

In Fig. 13 we consider a portion of a Facebook social network [28] and we plot the equilibrium reached in opinions. The behavior of the network heavily depends on the initial state of opinions. With the same parameters but a different initial condition, the coupled system can reach a limit cycle or exhibit chaotic behavior (please check videolimitcycle and videochaos). Notably, FSO is rarely observed in simulations, likely due to the topological clustering inherent to community-based friend networks.

These observations confirm that the behaviors noted previously can occur in diverse small-world network structures, not limited by the regularity or specific topology of the graphs.

Remark 5. While not explicitly demonstrated in this section, it is important to note that these dynamical behaviors (FSO, convergence to one equilibrium, limit cycles, and chaotic patterns) are not unique to the specific signals used in the presented examples. Similar behaviors can be replicated with a variety of other signaling functions for both

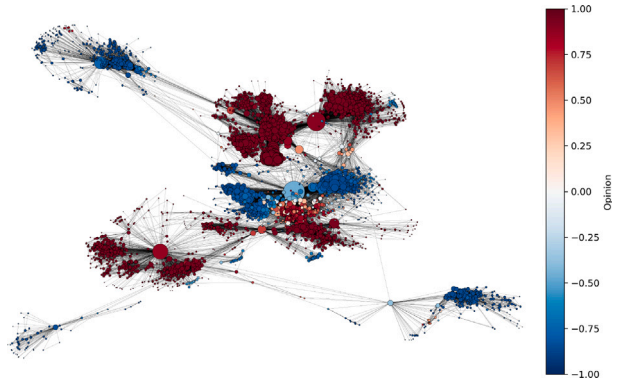


Fig. 13. Facebook Network graph, representing anonymized users within ten friend lists. Edges correspond to friendships. The graph contains 4039 nodes and has a diameter of 8. For more details, see [29]. The displayed opinions are at equilibrium for $s_\theta = s_p = s$ with $\delta = 0.05$. Parameters: $\beta = 0.1$, $\gamma = 0.2$, and $\bar{p} = 25{,}000$. Initial conditions: $p(0) = 23{,}750$ and $\boldsymbol{\theta}(0)$ as i.i.d. random uniform variables on $[-1, 1]$, except for biased clusters at top-left and bottom-right around $\theta = -0.95$.

opinions and atmospheric pollution. This indicates that the underlying dynamics of the system are robust to changes in the way agents interact and respond to the air pollution dynamics, suggesting a broad applicability of our findings across different types of network-driven processes.

6. Conclusion

In this paper, we have introduced and analyzed a nonlinear opinion dynamics model coupled with an external signal. Specifically, we consider that the external dynamics represent a very simple pollution model in which the emission level depends on the emissions of the individuals in the social network. Conversely, opinions are influenced by both the signal from their neighbors and the pollution level. We have shown that different behaviors are possible, ranging from convergence to a steady state to a chaotic behavior of the coupled dynamics. The chaotic regime is usually characterized by a strange attractor and numerical simulations demonstrate fractal patterns. Another interesting phenomenon observed is that of chaotic de-synchronization, where agents that synchronize in limit cycles or equilibria get de-synchronized due to the chaotic behavior.

CRediT authorship contribution statement

Anthony Couthures: Writing – review & editing, Writing – original draft, Software, Investigation, Formal analysis. **Vineeth Satheeskumar Varma:** Writing – review & editing, Supervision. **Samson Lasaulce:** Supervision. **Irinel - Constantin Morărescu:** Writing – review & editing, Validation, Supervision.

Declaration of competing interest

The authors declare that they have no known competing financial interests or personal relationships that could have appeared to influence the work reported in this paper.

Acknowledgments

The work of S. Lasaulce was supported by UAE TII 6G Chair on Native AI.

Data availability

No data was used for the research described in the article.

References

[1] Ising E. Contribution to the theory of ferromagnetism. (Ph.D. thesis), University of Hamburg; 1924.

[2] Sznajd-Weron K, Sznjad J. Opinion evolution in closed community. Internat J Modern Phys C 2000;11(6):1157–65.

[3] Deffuant G, Neau D, Amblard F, Weisbuch G. Mixing beliefs among interacting agents. Adv Complex Syst 2000;3:87–98.

[4] Hegselmann R, Krause U. Opinion dynamics and bounded confidence models, analysis, and simulation. J Artif Soc Soc Simul 2002;5(3).

[5] Friedkin NE, Johnsen EC. Social influence and opinions.. J Math Sociol 1990;15:193–206.

[6] Morărescu I-C, Girard A. Opinion dynamics with decaying confidence: Application to community detection in graphs. IEEE Trans Autom Control 2011;56(8):1862–73.

[7] DeGroot MH. Reaching a consensus. J Amer Statist Assoc 1974;69(345):118–21.

[8] Altafini C. Consensus problems on networks with antagonistic interactions. IEEE Trans Autom Control 2013;58(4):935–46.

[9] Martins A and. Continuous opinions and discrete actions in opinion dynamics problems. Internat J Modern Phys C 2008;19(4):617–25.

[10] Chowdhury NR, Morărescu I-C, Martin S, Srikant S. Continuous opinions and discrete actions in social networks: a multi-agent system approach. In: Proceedings 55th IEEE conference on decision and control. 2016, p. 1739–44.

[11] Ceragioli F, Frasca P. Consensus and disagreement: The role of quantized behaviors in opinion dynamics. SIAM J Control Optim 2018;56(2):1058–80.

[12] Hofmann DJ, Butler JH, Tans PP. A new look at atmospheric carbon dioxide. Atmos Environ 2009;43(12):2084–6. http://dx.doi.org/10.1016/j.atmosenv.2008.12.028.

[13] Joos F, Roth R, Fuglestvedt JS, Peters GP, Enting IG, von Bloh W, et al. Carbon dioxide and climate impulse response functions for the computation of greenhouse gas metrics: A multi-model analysis. Atmos Chem Phys 2013;13(5):2793–825. http://dx.doi.org/10.5194/acp-13-2793-2013.

[14] Leach N, Jenkins S, Nicholls Z, Smith C, Lynch J, Cain M, Walsh T, Wu B, Tsutsui J, Allen M. FaIRv2.0.0: A generalized impulse response model for climate uncertainty and future scenario exploration. Geosci Model Dev 2021;14:3007–36. http://dx.doi.org/10.5194/gmd-14-3007-2021.

[15] Garg A, Kumar A, Gupta NC. Comprehensive study on impact assessment of lockdown on overall ambient air quality amid COVID-19 in Delhi and its NCR, India. J Hazard Mater Lett 2021;2:100010.

[16] Bizyaeva A, Franci A, Leonard NE. Nonlinear Opinion Dynamics With Tunable Sensitivity. IEEE Trans Autom Control 2023;68(3):1415–30.

[17] He Z, Lai X. Bifurcation and chaotic behavior of a discrete-time predator–prey system. Nonlinear Anal Real World Appl 2011;12(1):403–17.

[18] Lin Y, Din Q, Rafaqat M, Elsadany AA, Zeng Y. Dynamics and chaos control for a discrete-time Lotka–Volterra model. IEEE Access 2020.

[19] Weitz JS, Eksin C, Paarporn K, Brown SP, Ratcliff WC. An oscillating tragedy of the commons in replicator dynamics with game-environment feedback. Proc Natl Acad Sci 2016;113(47):E7518–25. http://dx.doi.org/10.1073/pnas.1604096113.

[20] Tilman AR, Plotkin JB, Akçay E. Evolutionary games with environmental feedbacks. Nature Commun 2020;11(1):915. http://dx.doi.org/10.1038/s41467-020-14531-6.

[21] Frieswijk K, Zino L, Cao M, Morse AS and. Modeling the co-evolution of climate impact and population behavior: A mean-field analysis⋆. IFAC-PapersOnLine 2023;56(2):7381–6. http://dx.doi.org/10.1016/j.ifacol.2023.10.355.

[22] Couthures A, Mongaillard T, Varma VS, Lasaulce S, Morărescu I-C. Analysis of a continuous opinion and discrete action model coupled with an external dynamics. In: 2024 European control conference. ECC, 2024, p. 3392–7. http://dx.doi.org/10.23919/ECC64448.2024.10591291.

[23] Granas A, Dugundji J. Fixed point theory, springer monographs in mathematics. New York, NY: Springer New York; 2003.

[24] Veerman JJP, Lyons R. A primer on Laplacian dynamics in directed graphs. 2020, arXiv:2002.02605.

[25] Kokotović P, Khalil H, O'Reilly J. Singular perturbation methods in control: analysis and design. SIAM; 1999.

[26] Hagberg AA, Schult DA, Swart PJ. Exploring network structure, dynamics, and function using NetworkX. In: G. Varoquaux J Millman, editor. Proceedings of the 7th python in science conference. Pasadena, CA USA; 2008, p. 11–5. http://dx.doi.org/10.25080/TCWV9851.

[27] Girvan M, Newman MEJ. Community structure in social and biological networks. Proc Natl Acad Sci 2002;99(12):7821–6.

[28] Leskovec J, Mcauley J. Learning to discover social circles in ego networks. In: Pereira F, Burges C, Bottou L, Weinberger K, editors. Advances in neural information processing systems. vol. 25, Curran Associates, Inc.; 2012.

[29] NetworkX. 2024, https://github.com/networkx/nx-guides.